Clinical Science (2018) **132** 1565–1580
https://doi.org/10.1042/CS20180435

PORTLAND PRESS

Research Article

LTBP2 is secreted from lung myofibroblasts and is a potential biomarker for idiopathic pulmonary fibrosis

Yasunori Enomoto[1,2], Sayomi Matsushima[1,2], Kiyoshi Shibata[3], Yoichiro Aoshima[1,2], Haruna Yagi[1], Shiori Meguro[1], Hideya Kawasaki[1], Isao Kosugi[1], Tomoyuki Fujisawa[2], Noriyuki Enomoto[2], Naoki Inui[2,4], Yutaro Nakamura[2], Takafumi Suda[2] and Toshihide Iwashita[1]

[1]Department of Regenerative and Infectious Pathology, Hamamatsu University School of Medicine, Shizuoka, Japan; [2]Second Division, Department of Internal Medicine, Hamamatsu University School of Medicine, Shizuoka, Japan; [3]Department of Advanced Research Facilities and Services, Hamamatsu University School of Medicine, Shizuoka, Japan; [4]Department of Clinical Pharmacology and Therapeutics, Hamamatsu University School of Medicine, Shizuoka, Japan

Correspondence: Yasunori Enomoto (enomotoy@hama-med.ac.jp) or Toshihide Iwashita (toshiiwa@hama-med.ac.jp)

Although differentiation of lung fibroblasts into α-smooth muscle actin (αSMA)-positive myofibroblasts is important in the progression of idiopathic pulmonary fibrosis (IPF), few biomarkers reflecting the fibrotic process have been discovered. We performed microarray analyses between FACS-sorted steady-state fibroblasts (lineage (CD45, TER-119, CD324, CD31, LYVE-1, and CD146)-negative and PDGFRα-positive cells) from untreated mouse lungs and myofibroblasts (lineage-negative, Sca-1-negative, and CD49e-positive cells) from bleomycin-treated mouse lungs. Amongst several genes up-regulated in the FACS-sorted myofibroblasts, we focussed on *Ltbp2*, the gene encoding latent transforming growth factor-β (TGF-β) binding protein-2 (LTBP2), because of the signal similarity to *Acta2*, which encodes αSMA, in the clustering analysis. The up-regulation was reproduced at the mRNA and protein levels in human lung myofibroblasts induced by TGF-β1. LTBP2 staining in IPF lungs was broadly positive in the fibrotic interstitium, mainly as an extracellular matrix (ECM) protein; however, some of the αSMA-positive myofibroblasts were also stained. Serum LTBP2 concentrations, evaluated using ELISA, in IPF patients were significantly higher than those in healthy volunteers (mean: 21.4 compared with 12.4 ng/ml) and showed a negative correlation with % predicted forced vital capacity ($r = -0.369$). The Cox hazard model demonstrated that serum LTBP2 could predict the prognosis of IPF patients (hazard ratio for death by respiratory events: 1.040, 95% confidence interval: 1.026–1.054), which was validated using the bootstrap method with 1000-fold replication. LTBP2 is a potential prognostic blood biomarker that may reflect the level of differentiation of lung fibroblasts into myofibroblasts in IPF.

Introduction

Idiopathic pulmonary fibrosis (IPF), pathologically known as usual interstitial pneumonia (UIP), is one of the most common interstitial lung diseases and has a poor prognosis [1]. Although the pathophysiology of lung fibrosis remains unclear, the currently accepted mechanism involves recurrent or repeated alveolar epithelial injuries; modulation by profibrotic cytokines, including transforming growth factor-β (TGF-β); activation and proliferation of fibroblasts; and the differentiation of fibroblasts into myofibroblasts, resulting in excessive production of extracellular matrix (ECM) proteins and aberrant fibrosis [2-4]. Amongst these, the differentiation of fibroblasts into myofibroblasts via the Smad and Akt signaling pathways is thought to be the main driving factor of lung fibrogenesis [5,6].

The clinical course of IPF is heterogeneous and often unpredictable [1]. Although pulmonary function parameters, including forced vital capacity (FVC), diffusion capacity for carbon monoxide (DLCO), and

Received: 28 May 2018
Revised: 03 July 2018
Accepted: 10 July 2018

Accepted Manuscript Online: 13 July 2018
Version of Record published: 31 July 2018

Clinical Science (2018) **132** 1565–1580
https://doi.org/10.1042/CS20180435

the scoring system based on these parameters are reliable biomarkers for IPF [1,7], measuring or re-evaluating these parameters is occasionally difficult in certain situations, such as for ventilated patients and patients with poor general health. Therefore, blood biomarkers that are easy to evaluate and are predictive of disease severity and/or prognosis are helpful in clinical settings.

To date, several blood biomarker candidates have been proposed for IPF, including Krebs von den Lungen-6 (KL-6), surfactant protein A and D, matrix metalloproteinase 1 and 7, CC chemokine ligand 18, C-X-C motif chemokine 13, and their combinations [8-11], but few have been sufficiently validated. Additionally, to our knowledge, no biomarker has been identified that reflects the essential fibrotic process 'differentiation of lung fibroblasts into myofibroblasts'. Although myofibroblasts are generally defined as fibroblasts up-regulating α-smooth muscle actin (αSMA) expression, the αSMA, an intracellular protein, is not measurable as a blood biomarker. Therefore, there is a need to find another protein that is excessively secreted into blood during fibroblast differentiation. Based on this context and our preclinical findings, in the present study, we focussed on a secreted protein, latent TGF-β binding protein-2 (LTBP2), and aimed to evaluate the potential of LTBP2 as a novel blood biomarker for IPF.

Material and methods

Mouse experiments and intratracheal administration of bleomycin

C57BL/6 male mice, aged 11–14 weeks and weighing 25–28 g, were purchased from Japan SLC. The mice were maintained in a pathogen-free mouse facility at our institution. All *in vivo* experiments complied with the Animal Research: reporting *in vivo* Experiments guidelines and were performed in accordance with the National Institute of Health Guide for the Care and Use of Laboratory Animals. In addition, the protocol of these *in vivo* experiments was approved by the Animal Care and Use Committee of Hamamatsu University School of Medicine (approval number: 2015008).

Mice were anesthetized and then intratracheally administered with a single microspray (MicroSprayer, Penn-Century, U.S.A.) of 3 mg/kg bleomycin sulphate (Wako, Japan) in 50 μl saline to induce lung fibrosis. Mice were killed on day 10–14, an early fibrotic stage, and the harvested lungs were dissociated for FACS or used for immunostaining.

Tissue dissociation of mouse lungs

After perfusion of the lungs with 5 ml DPBS (Gibco, U.S.A.) via the right ventricle and removal of the bronchus and pulmonary vessels, lungs were harvested and incubated with 200 U/ml collagenase type 2 (Worthington, U.S.A.) and 100 U/ml DNase 1 (Worthington, U.S.A.) for 30 min at 37°C in DPBS. Digested lung tissues were then cut using a gentleMACS Dissociator (Miltenyi Biotechnology, Germany) according to the manufacturer's instructions, and cells were filtered through a nylon screen (BD Biosciences, U.S.A.) to remove cell/tissue aggregates. The resulting single cell suspension was centrifuged and rinsed twice with FACS buffer (1% HEPES buffer, 2% heat-inactivated FBS, 120 μg/ml penicillin, 100 μg/ml streptomycin in HBSS).

FACS protocol

Mouse lung cells were incubated with antibodies against the following lineage-specific cell surface markers: CD45, TER-119, CD324 (E-cadherin), CD31, LYVE-1, and CD146. When isolating steady-state fibroblasts from untreated mice, anti-PDGFRα (CD140a) antibody was added. In contrast, for isolation of activated fibroblasts and myofibroblasts from bleomycin-treated mice, anti-Sca-1 and biotin-conjugated anti-CD49e (integrin α5) antibodies were added. Incubation with these antibodies was performed on ice for 60 min. After centrifugation and rinsing twice in FACS buffer, only for the bleomycin-treated mouse lung cells, incubation with streptavidin for 60 min on ice was additionally done. Based on the results of our previous study but with a few modifications [12], we defined steady-state fibroblasts as lineage-negative and PDGFRα-positive cells from untreated mouse lungs; activated fibroblasts as lineage-negative and Sca-1-positive cells from bleomycin-treated mouse lungs; and myofibroblasts as lineage-negative, Sca-1-negative, and CD49e-positive cells from bleomycin-treated mouse lungs (Figure 1A). On the contrary, each lineage-specific cell surface marker (CD45, CD324, CD31, LYVE-1, and CD146) was also used for the isolation of blood cells, epithelial cells, vascular endothelial cells, lymphatic endothelial cells, and smooth muscle cells, respectively. Before sorting, Sytox-Red or -Green (1:1000; Molecular Probes, U.S.A.) was used to remove the dead cells.

The protein level of intracellular αSMA, a myofibroblast marker, was quantitated by permeabilizing 3000 isolated fibroblasts/myofibroblasts using IntraPrep (Beckman Coulter, U.S.A.), according to the manufacturer's instructions. After centrifugation and rinsing in DPBS, the cells were incubated with anti-αSMA antibody for 60 min at room temperature. After additional centrifugation and rinsing in DPBS, fluorescence intensities of FITC-conjugated

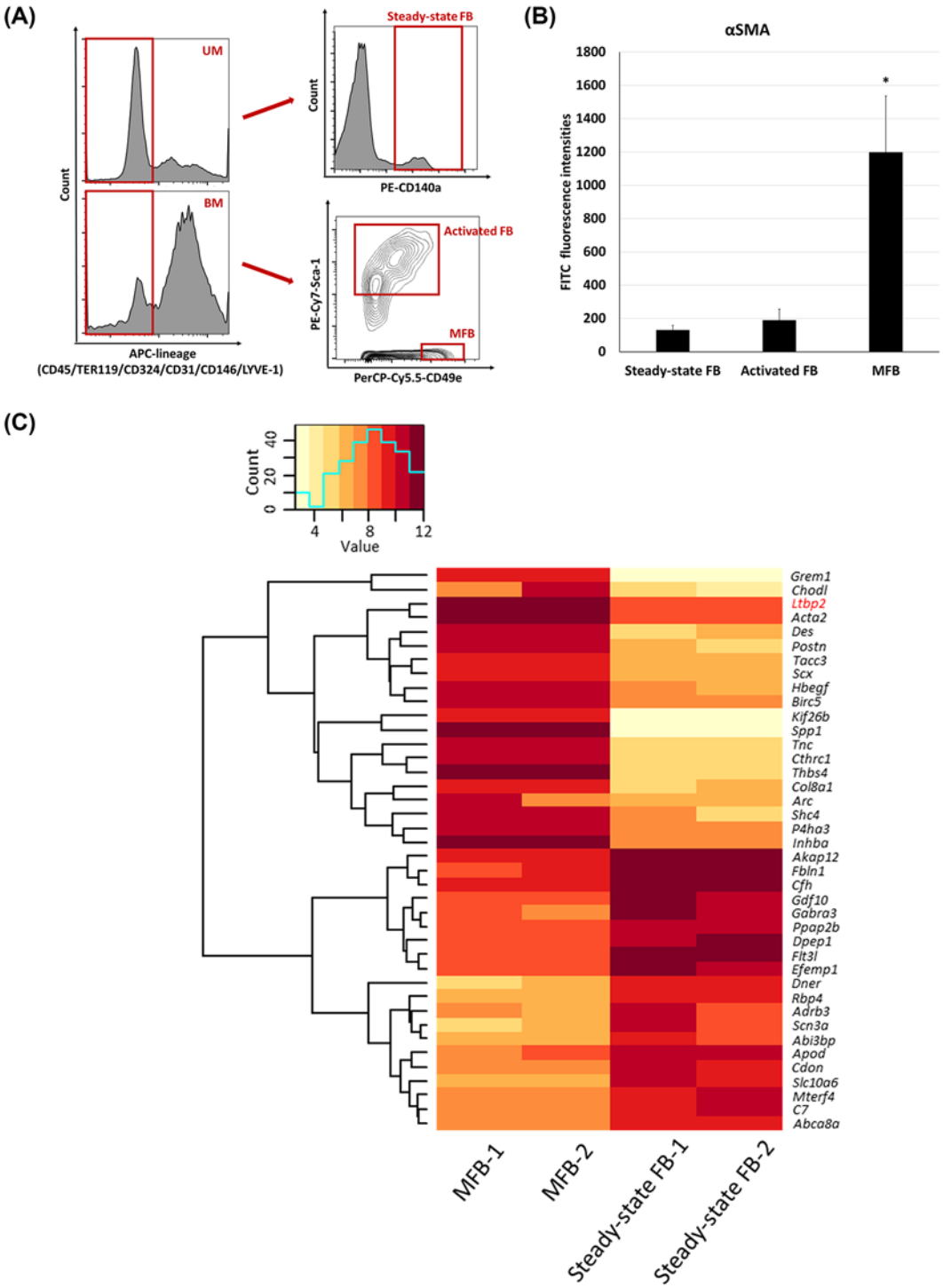

Figure 1. FACS and microarray analyses

(**A**) Representative images of FACS analysis for steady-state fibroblasts (FB) from untreated mice (UM) and activated FB/myofibroblasts (MFB) from bleomycin-treated mice (BM). (**B**) Fluorescence intensities of FITC-conjugated anti-αSMA antibody in steady-state FB, activated FB, and MFB (n=4 per group). Statistical comparisons by t test were performed using the value of steady-state FB as a control. *P<0.05. (**C**) Heatmap generated by microarray analyses. Genes up-regulated in MFB were selected according to the following criteria: (i) five-fold greater than in steady-state FB; (ii) five-fold greater than in total lung homogenates; and (iii) two-fold greater than the mean value of all genes in MFB. Conversely, genes up-regulated in steady-state FB were defined according to the following criteria: (i) five-fold greater than in MFB; (ii) five-fold greater than in total lung homogenates; and (iii) two-fold greater than the mean value of all genes in steady-state FB. The listed genes are the top 20 genes with high signals in each group and are available in the NCBI Reference Sequence.

Clinical Science (2018) **132** 1565–1580
https://doi.org/10.1042/CS20180435

anti-αSMA antibody in steady-state fibroblasts, activated fibroblasts, and myofibroblasts were measured for confirmation (Figure 1B).

The antibodies and their concentrations used in FACS are listed in Supplementary Table S1. Isotype antibodies were used for setting cut-off levels. To obtain a high purity, the samples were subjected to sorting twice. All sorting and analyses were performed using FACSAria (BD Biosciences, U.S.A.). FACS data were analyzed using FlowJo software version 7.6.5 (Tree Star, U.S.A.).

Microarray analyses for steady-state fibroblasts and myofibroblasts isolated from mouse lungs

Total RNA was extracted from two independently prepared batches of 50000 cells of steady-state fibroblasts, myofibroblasts, or lung homogenates (as a control). Additionally, RNA was amplified using the Ovation Pico WTA System V2 (NuGEN Technologies, U.S.A.). Gene expression profiling was commissioned to an outside agency (SurePrint G3 Mouse Gene Expression 8x60K v2 Microarray, Takara Bio, Japan). The experiments and description followed the MIAME guidelines; the raw data are available at the GEO database (accession number: GSE111043). The heatmaps of gene expression profiles are shown in Figure 1C and in Supplementary Figure S1; genes that were up-regulated or down-regulated in myofibroblasts and the ontology profiles are summarized in Supplementary Tables S2 and S3, respectively. RNA levels of several genes were confirmed using reverse transcription-PCR (RT-PCR).

Quantitative RT-PCR for lung fibroblasts and myofibroblasts

Total RNA was extracted from freshly isolated mouse cells or cultured human cells using TRIzol (Invitrogen, U.S.A.) with glycogen as a carrier. RNA was extracted as per the manufacturer's instructions. Extracted RNA was treated with RNase free DNase 1 (Ambion, U.S.A.) in the presence of RNase Inhibitor (Invitrogen, U.S.A.) for 10 min at 37°C. RNA was purified using the RNeasy Mini Kit (Qiagen, Germany) according to the manufacturer's instructions. After first-strand cDNA was synthesized using SuperScript Reverse Transcriptase (Invitrogen, U.S.A.) with random primers (Invitrogen, U.S.A.), cDNA equivalent to 100 cells was used for each PCR. Gene-specific primers were designed using Primer 3 software (v.0.4.0) to generate short amplicons (100–150 bp). PCR was performed using the SYBR Green quantitative RT-PCR (qRT-PCR) Kit (Applied Biosystems, U.S.A.). The PCR cycling program comprised 1 cycle at 95°C for 10 min, 40 cycles at 95°C for 15 s and 60°C for 1 min, and 1 cycle at 95°C for 15 s and 60°C for 1 min (ABI StepOnePlus, Applied Biosystems, U.S.A.). The cycle threshold (C_T) for each gene was measured, and the values were expressed as $2^{-\Delta CT}$ (ΔC_T: C_T of target gene minus C_T of glyceraldehyde-3-phosphate dehydrogenase). Primer sequences for RT-PCR are listed in Supplementary Table S4.

Experiments using human lung fibroblasts

Primary human adult lung fibroblasts (HPF-a #3310, passage number: less than three) were purchased from the ScienCell Research Laboratories (U.S.A.). In addition, primary human fetal lung fibroblasts (TIG-1-20, passage number: unknown) were also purchased from the Japanese Collection of Research Bioresources Cell Bank (Japan). These fibroblasts were grown on a 24-well plate to confluence in growth medium containing DMEM (Gibco, U.S.A.), 10% FBS, 2 mM glutamine, and a 1:1000 dilution of antibiotics solution. Cells were maintained in an incubator at 37°C in a 5% CO_2 atmosphere. Confluent monolayers were washed twice with DPBS. The medium was then replaced with chemically defined serum-free medium (Lonza, U.S.A.) containing recombinant human TGF-β1 (#0117209-1, PeproTech, U.S.A.) at concentrations of 0, 2.5, or 5 ng/ml. After incubation for 48 h, the culture supernatant was collected and used for ELISA according to the manufacturer's protocol (SEB630Hu, Cloud-Clone, U.S.A.). Cells were collected from the plates for RT-PCR.

Selection of patients with IPF

A retrospective database review at Hamamatsu University Hospital between 2000 and 2014 identified 152 IPF patients based on the criteria used in a recent clinical trial [13]. Amongst these patients, 36 patients who had or developed malignant diseases such as lung cancer and prostate cancer within 6 months from IPF diagnosis were excluded because their clinical course and serum concentrations of LTBP2 would likely be affected by the malignancies [14–22]. Subsequently, 116 IPF patients were included in the present study. The patients' medical records were reviewed to obtain the clinical data and the clinical course, including prognosis (deaths by all causes or respiratory events) and complications of acute exacerbation of IPF [23]. The present study was approved by the Institutional Review Board of Hamamatsu University School of Medicine (approval number: 15-197).

Serum sampling and measurement of LTBP2 concentrations

Serum samples were obtained at the time of IPF diagnosis and stored at −80°C for future analysis. Written informed consent regarding serum conservation was obtained from all patients (approval number: 15-165). As a control, serum samples were also collected from 31 healthy volunteers who worked or had worked at Hamamatsu University School of Medicine. Serum LTBP2 concentrations were quantitated using ELISA (SEB630Hu, Cloud-Clone, U.S.A.).

Immunohistochemistry and immunofluorescence

Lung specimens were obtained from three untreated mice, three bleomycin-treated mice (killed on day 10–14), ten patients with IPF (extracted by surgical lung biopsy), a patient who died of acute exacerbation of IPF (extracted by autopsy), and two patients with spontaneous pneumothorax and early-stage lung cancer, respectively, as normal controls (extracted by lung resection).

These lung specimens had been fixed in 10% formalin and embedded in paraffin. Deparaffinized sections (4-μm-thick) were preheated to 120°C for 15 min (pH = 6). After inactivating endogenous peroxidase with 0.3% H_2O_2 for 10 min, the sections were incubated with blocking solution (10% goat serum in PBS and 0.1% Triton X-100 in PBS) for 10 min and then incubated with anti-LTBP2 antibody (1:1000; Proteintech, U.S.A.) or anti-αSMA antibody (1:300; Dako, U.S.A.) as a primary antibody for 1 h.

Immunohistochemistry

Lung sections were incubated with peroxidase-labeling goat anti-rabbit IgG antibody (Nichirei Biosciences, Japan) for 15 min. The immunoreaction was visualized using 3,3′-diaminobenzidine (Dako, U.S.A.) and then counterstained with Hematoxylin. Hematoxylin–Eosin staining and Elastica van Gieson staining were also performed on other serial sections.

Immunofluorescence

In addition to the anti-LTBP2 antibody and anti-αSMA antibody, for human lung sections, anti-CD45 antibody (1:100; Dako, U.S.A.), anti-CD324 antibody (1:20; Dako, U.S.A.), anti-CD31 antibody (1:100; Dako, U.S.A.), anti-podoplanin antibody (1:200; Dako, U.S.A.), and anti-h-caldesmon antibody (1:5; MyBioSource, Canada), anti-elastin antibody (1:500; Abcam, U.S.A.), and anti-fibrillin-1 antibody (1:200; EMD Millipore, U.S.A.) were also used as primary antibodies. The sections were incubated with Hoechst 33342 (1:1000; Sigma, U.S.A.) with Alexa fluor conjugated secondary antibodies for 30 min. The sections were visualized using a confocal microscope (Leica, U.S.A.). In the present study, human lung myofibroblasts in immunofluorescence images were defined as single cells with positivity for αSMA and negativity for lineage markers: CD45 (blood cells), CD324 (epithelial cells), CD31 (vascular endothelial cells), podoplanin (lymphatic endothelial cells), and h-caldesmon (smooth muscle cells).

Statistical analysis

For *in vitro* experiments, data were expressed as mean ± S.E.M.; group comparisons with each control were performed using the Student's *t* test. For analyses using human materials, data were described as number (%) or median (interquartile range) unless otherwise noted; group comparisons were performed using Fisher's exact test or the Mann–Whitney U test. Using the curve of receiver operating characteristic (ROC) and the Youden index method, a cut-off value with favorable sensitivity and specificity was calculated to discriminate patients with IPF from healthy controls. Spearman's rank correlation coefficients were evaluated between serum LTBP2 concentrations and the other clinical factors. Overall survival was defined as the time from the date of IPF diagnosis to the date of censoring or death (by all causes or respiratory events). Patients were censored if they remained alive until 31 December 2016 or if they dropped out of the follow-ups. The Cox proportional hazard model was used to evaluate the prognostic impact of serum LTBP2 concentrations. Additionally, the bootstrap method with 1000-fold replication was utilized for estimating variability of hazard ratios of serum LTBP2 concentrations [24]. To estimate the ideal cut-off value of serum LTBP2 concentrations in patients with IPF, a time-dependent ROC analysis was performed [25]. The survival curves were generated using the Kaplan–Meier method and compared using log-rank test. Statistical analyses were performed using R software version 2.15.1 (the R Foundation for Statistical Computing, Austria) and SPSS software version 13.0 (SPSS, U.S.A.). $P<0.05$ was considered significant.

Clinical Science (2018) **132** 1565–1580
https://doi.org/10.1042/CS20180435

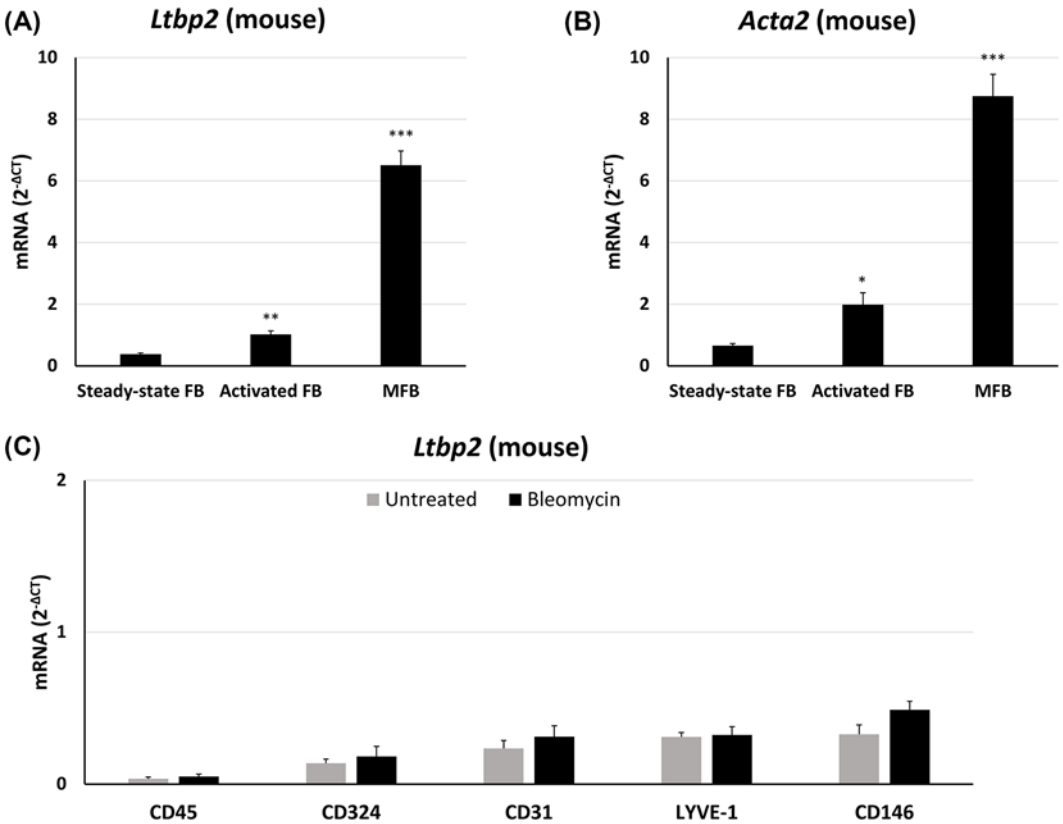

Figure 2. Results of RT-PCR using mouse lung cells isolated by FACS

(**A**,**B**) *Ltbp2* and *Acta2* mRNA levels in mouse lung steady-state fibroblasts (FB), activated FB, and myofibroblasts (MFB) (n=3 per group). Statistical comparisons by t test were performed using the value of steady-state FB as a control. $^{*}P<0.05$, $^{**}P<0.01$, $^{***}P<0.001$. (**C**) *Ltbp2* mRNA levels in lineage cells from untreated and bleomycin-treated mouse lungs (n=3 per group). There were no statistically significant differences between the two mouse groups (t test).

Results

Ltbp2 was up-regulated in bleomycin-induced activated fibroblasts and myofibroblasts isolated from mouse lungs

Microarray comparisons between FACS-sorted steady-state fibroblasts and myofibroblasts from mouse lungs revealed 44 genes that were highly up-regulated in myofibroblasts at the transcriptional level based on our criteria (Supplementary Table S2). These genes were commonly annotated with 'ECM' or 'proteinaceous ECM' (Supplementary Table S3). Amongst them, we selected one gene, *Ltbp2*, because it encodes an extracellular protein and its signal was most similar to *Acta2*, a gene encoding αSMA, in the clustering analysis (Figure 1C). Consistent with the microarray results, qRT-PCR analyses confirmed that the *Ltbp2* mRNA levels were significantly higher in myofibroblasts than in steady-state fibroblasts (Figure 2A). Intermediate *Ltbp2* mRNA levels were observed in bleomycin-induced activated fibroblasts. These differences in *Ltbp2* mRNA levels seemed parallel to *Acta2* mRNA levels (Figure 2B). On the other hand, the *Ltbp2* mRNA levels in CD45-positive blood cells, CD324-positive epithelial cells, CD31-positive vascular endothelial cells, LYVE-1-positive lymphatic endothelial cells, and CD146-positive smooth muscle cells (pericytes and endothelial cells) were commonly low and not significantly different between untreated and bleomycin-treated mouse lungs (Figure 2C), suggesting that these lineage cells were not the main source of LTBP2 in mouse lungs.

LTBP2 was up-regulated in TGF-β1-induced myofibroblasts in human lungs

To determine whether the results in mouse cells were reproducible in human cells, we analyzed the *LTBP2* mRNA levels in human lung fibroblasts with or without the stimulation by TGF-β1. As shown in Figure 3A,B, the TGF-β1 stimulation significantly up-regulated *LTBP2* mRNA levels, which almost corresponded to the change in *Acta2* mRNA

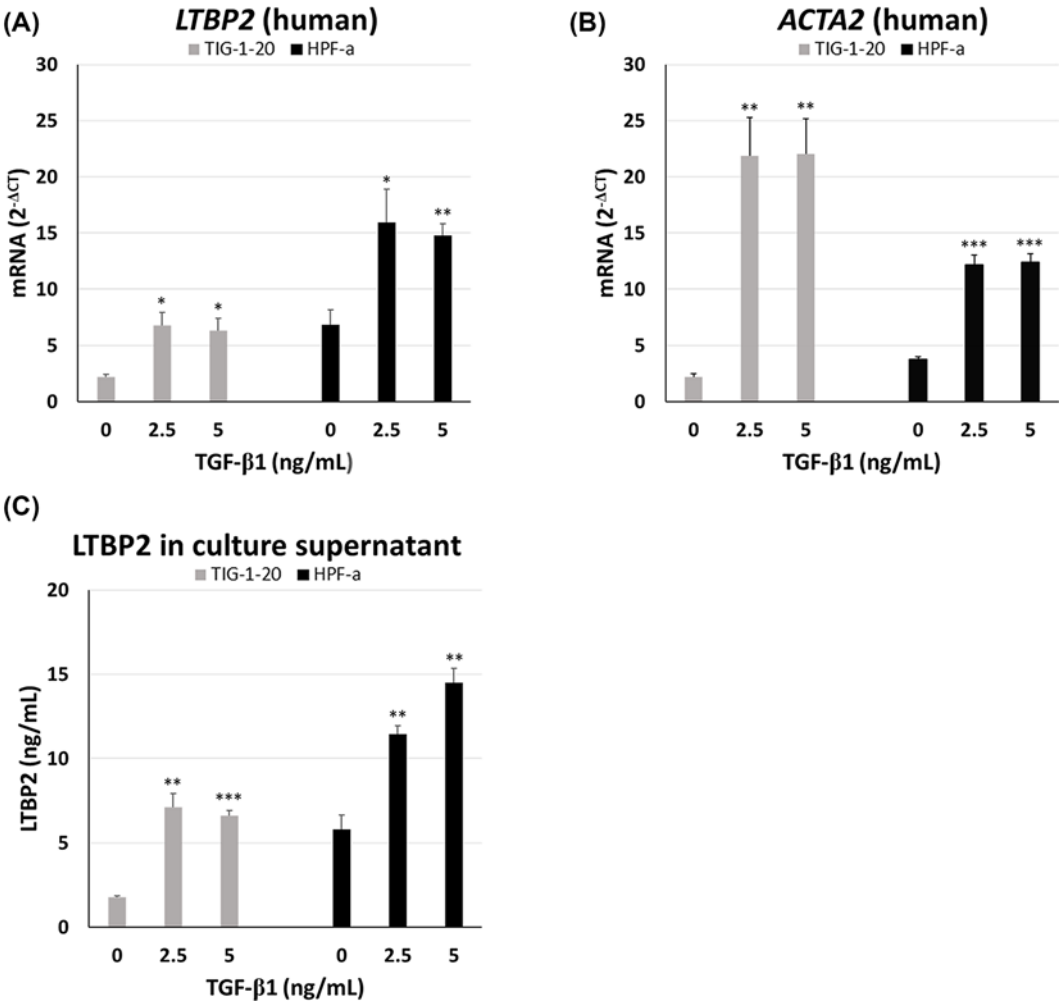

Figure 3. Results of RT-PCR and ELISA using human lung fibroblasts (TIG-1-20 and HPF-a)

(**A**,**B**) *LTBP2* and *Acta2* mRNA levels in human lung fibroblasts with or without 48-h external administration of TGF-β1 (n=3 per group). Statistical comparisons by t test were performed using the value of the untreated group as a control. *P<0.05, **P<0.01, ***P<0.001. (**C**) Protein concentrations, measured by ELISA, of LTBP2 in culture supernatant with or without 48-h external administration of TGF-β1 (n=3 per group). Statistical comparisons by t test were performed using the value of the untreated group as a control. *P<0.05, **P<0.01, ***P<0.001.

levels. In addition, protein concentrations of LTBP2 in culture supernatants, evaluated by ELISA, were significantly higher in TGF-β1-induced myofibroblasts than in controls, suggesting that the extracellular secretion of LTBP2 proteins was higher from TGF-β1-induced myofibroblasts than from untreated fibroblasts (Figure 3C).

Localization of LTBP2 in normal and fibrotic lungs

Figure 4 shows the results of immunohistochemistry. In normal lung sections, scarce positivity was observed except at the peribronchovascular lesions (Figure 4A,B). In contrast, LTBP2 staining was broadly positive in the fibrotic interstitium in biopsied IPF lungs. Unexpectedly, the bodies of fibroblastic foci, which are thought to be aggregated myofibroblasts, were not clearly positive for LTBP2 staining (Figure 4C–F). Elastica van Gieson staining showed that the distribution of LTBP2 partially overlapped with the elastic fibers (Figure 4G,H).

Consistent with the immunohistochemistry results, immunofluorescence staining for LTBP2 was extensively positive in the fibrotic interstitium but negative in the bodies of fibroblastic foci in biopsied IPF lungs (Figure 5A and Supplementary Figure S2A). However, some αSMA-positive myofibroblasts, which did not configure fibroblastic foci, stained positive for LTBP2 in the cytoplasm, suggesting that LTBP2 was secreted from the myofibroblasts (Figure 5B). These findings are consistent with the results seen in bleomycin-treated mouse lungs (Supplementary Figure S3). On

Clinical Science (2018) **132** 1565–1580
https://doi.org/10.1042/CS20180435

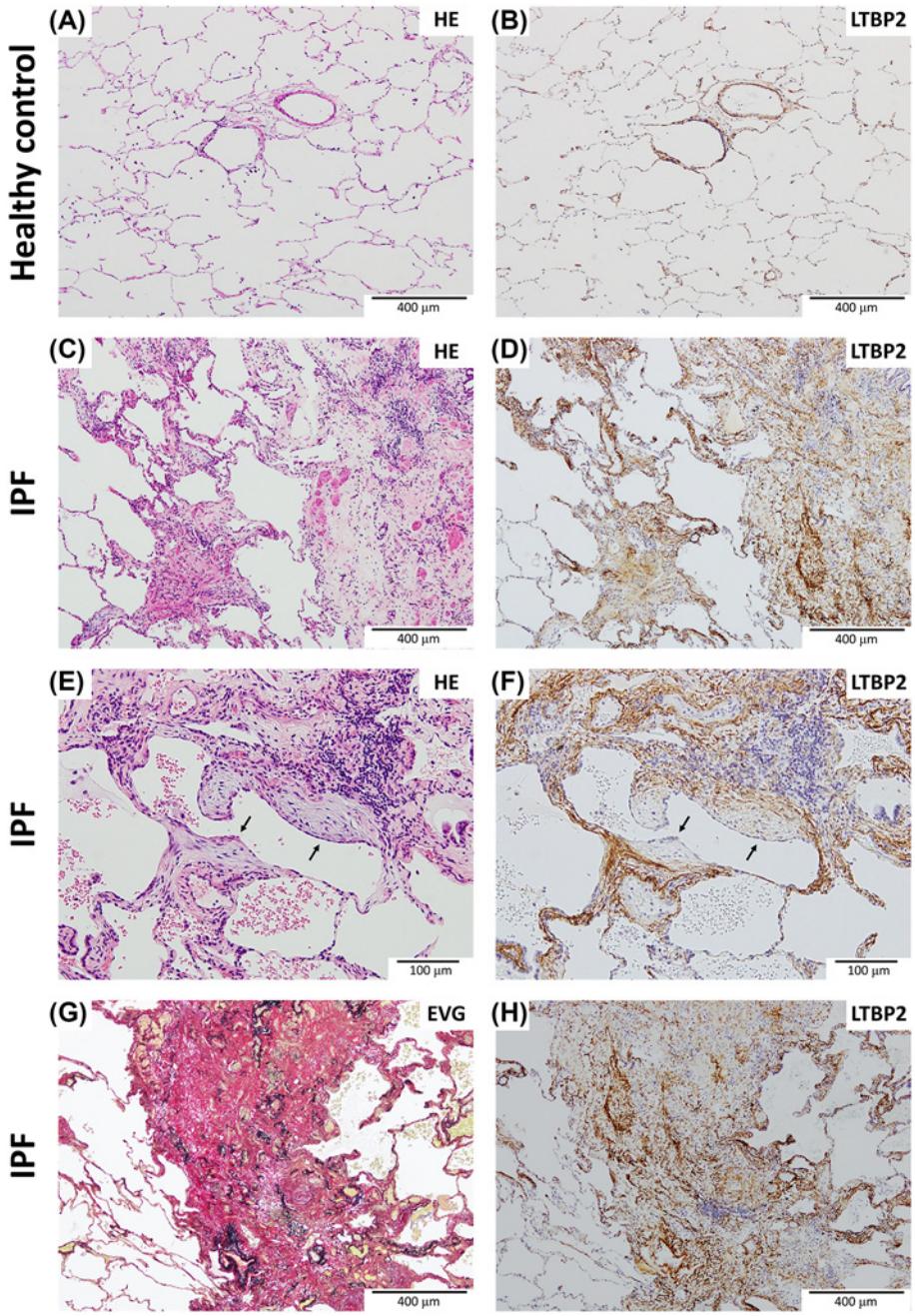

Figure 4. Representative immunohistochemistry images of lungs from a healthy subject and a patient with IPF who received surgical lung biopsy

(**A**,**B**) Lung section from a healthy subject, stained by Hematoxylin–Eosin (HE) and anti-LTBP2 antibody. (**C**–**F**) Images of fibrotic lesions in an IPF lung, stained by HE and anti-LTBP2 antibody. LTBP2 was broadly positive in the fibrotic interstitium but almost negative in the body of fibroblastic foci (arrows), as well as in epithelial cells, interstitial inflammatory cells, and alveolar macrophages. (**G**,**H**) Images of fibrotic lesions in an IPF lung, stained by Elastica van Gieson (EVG) and anti-LTBP2 antibody.

the contrary, LTBP2 staining was not observed in blood cells (CD45), epithelial cells (CD324), vascular endothelial cells (CD31), lymphatic endothelial cells (podoplanin), and vascular smooth muscle cells (h-caldesmon) (Figure 5C–F). In contrast, as an ECM protein, LTBP2 partially colocalized with elastin and fibrillin-1, which are major elastinogenesis-related proteins (Supplementary Figure S2B,C).

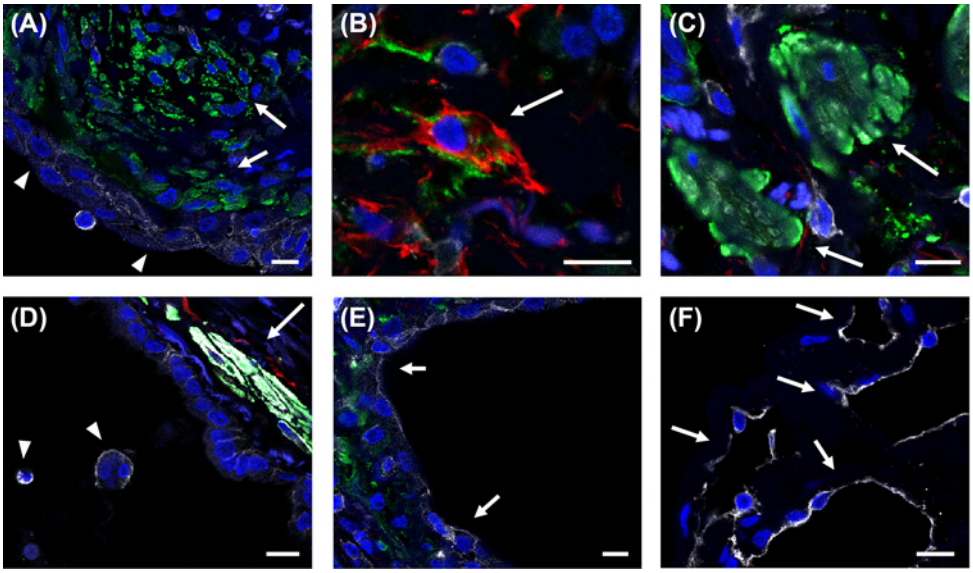

Figure 5. Representative immunofluorescence images of a biopsied lung of IPF (color: green = αSMA; red = LTBP2; white = lineage markers (CD45, CD324, CD31, podoplanin, and h-caldesmon))

(**A**) (Fibroblastic focus): aggregated αSMA-positive, LTBP2-negative, and lineage-negative myofibroblasts (arrows) and αSMA-negative, LTBP2-negative, and lineage (CD324)-positive epithelial cells (triangles). (**B**) (Fibrotic interstitium): a non-aggregated αSMA-positive, LTBP2-positive, and lineage-negative myofibroblast (arrow). (**C**) (Fibrotic interstitium): αSMA-positive, LTBP2-negative, and lineage (h-caldesmon)-positive smooth muscle cells at an alveolar wall (arrows). (**D**) (Bronchiole): αSMA-positive, LTBP2-negative, and lineage (h-caldesmon)-positive smooth muscle cells around a bronchiole (arrows); αSMA-negative, LTBP2-negative, and lineage (CD45)-positive alveolar macrophages (triangles). (**E**) (Blood vessel) αSMA-negative, LTBP2-negative, and lineage (CD31)-positive vascular endothelial cells (arrows). (**F**) (Lymphatic vessel): αSMA-negative, LTBP2-negative, and lineage (podoplanin)-positive lymphatic endothelial cells (arrows). All scale bars = 10 μm.

Table 1 Comparison of baseline characteristics between patients with IPF and healthy controls

	IPF *n*=116	Healthy controls *n*=31	*P*
Serum LTBP2, ng/ml	18.6 (15.4–23.0)	12.2 (9.4–14.4)	<0.001
Age, years	71 (66–77)	62 (58–76)	NS
Male	101 (87)	27 (81)	NS
Current or former smoker	96 (83)	NA	
Smoking dose (pack-year)	37 (14.5–60)	NA	
PaO_2 on room air (Torr)	76 (69–85)	NA	
% predicted FVC (%)	73 (58–87)	NA	
% predicted DLCO (%)	65 (50–83)	NA	
Serum KL-6 (U/ml)	988 (644–1510)	NA	
Serum SP-D (ng/ml)	222 (140–339)	NA	
Serum LDH (U/l)	235 (205–266)	NA	

Data are described as *n*(%) or median (interquartile range). All *P*-values were evaluated by Fisher's exact test or the Mann–Whitney U test as appropriate. Abbreviations: LDH, lactate dehydrogenase; NA, not available; NS, not significant; SP-D, surfactant protein-D.

Serum LTBP2 in patients with IPF

To evaluate the clinical significance of LTBP2, serum concentrations of LTBP2 in patients with IPF and healthy controls were analyzed using ELISA. Baseline characteristics are summarized in Table 1. Serum LTBP2 concentrations in patients with IPF were significantly higher than those in healthy controls (median: 18.6 ng/ml (mean: 21.4) compared with 12.2 ng/ml (mean: 12.4), $P<0.001$; Figure 6A). Figure 6B shows the ROC curve with an area under curve (AUC) of 0.862. The ideal cut-off value was calculated as 15.1 ng/ml; the sensitivity and specificity for discriminating patients with IPF from healthy controls were 78.4 and 87.1%, respectively. Additionally, as shown in Table 2, serum LTBP2

Clinical Science (2018) **132** 1565–1580
https://doi.org/10.1042/CS20180435

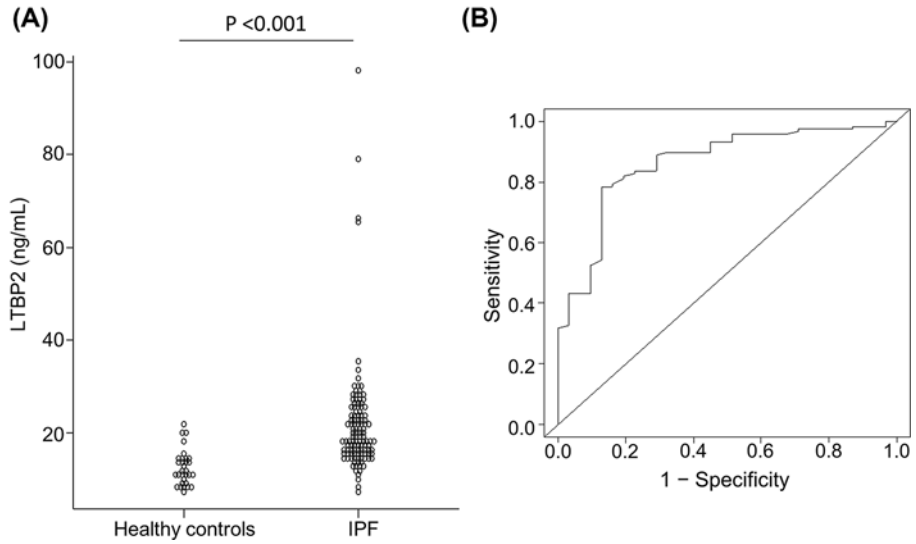

Figure 6. Serum LTBP2 concentrations evaluated by ELISA

(**A**) Comparison of serum LTBP2 concentrations between patients with IPF (n=116) and healthy controls (n=31). Statistical comparison was performed using the Mann–Whitney U test. (**B**) ROC curve to discriminate patients with IPF from healthy controls.

Table 2 Correlations of serum concentrations of LTBP2 with other clinical factors in patients with IPF

	Coefficient value	*P*
Age, years	0.288	<0.01
Smoking dose (pack-year)	−0.071	NS
PaO_2 on room air (Torr)	−0.248	<0.05
% predicted FVC (%)	−0.369	<0.01
% predicted DLCO (%)	−0.217	NS
Serum KL-6 (U/ml)	0.155	NS
Serum SP-D (ng/ml)	0.123	NS
Serum LDH (U/l)	0.144	NS

All *P*-values were evaluated using Spearman's rank correlation coefficient. Abbreviations: LDH, lactate dehydrogenase; NS, not significant; SP-D, surfactant protein-D.

concentrations in patients with IPF showed a significant negative correlation with % predicted FVC (r = −0.369).

LTBP2 in acute exacerbation of IPF

We next sought to study the association between LTBP2 and acute exacerbation of IPF. Interestingly, patients who had acute exacerbation of IPF at the time of IPF diagnosis or who developed the event within 6 months of their diagnosis, had significantly higher serum LTBP2 levels than the other patients (median: 21.4 ng/ml (mean: 29.0) compared with 17.9 ng/ml (mean: 19.4), P<0.01; Figure 7A). Immunostaining of autopsied lung sections from a patient who died of acute exacerbation of IPF revealed diffuse alveolar damage with a lot of αSMA-positive and non-fibroblastic foci myofibroblasts within the alveolar walls. Most of these myofibroblasts were stained or surrounded by LTBP2. In addition, interestingly, hyaline membranes in the alveolar spaces seemed to contain LTBP2 proteins (Figure 7B–F). In contrast with the biopsied lungs without acute exacerbation, LTBP2 positivity was also detected in or around proliferated smooth muscle cells at the fibrotic alveolar walls (Figure 7G). However, even with acute exacerbation, myofibroblasts configuring fibroblastic foci were not clearly stained by LTBP2.

Prognostic significance of serum LTBP2

The median follow-up period for patients with IPF was 36 months (interquartile range: 16–67 months). During the follow-up period, 60 of the 116 patients died (of which 55 died of respiratory events); no patients received lung transplantation; 16 patients became lost during follow up at least 6 months after IPF diagnoses. The Cox proportional

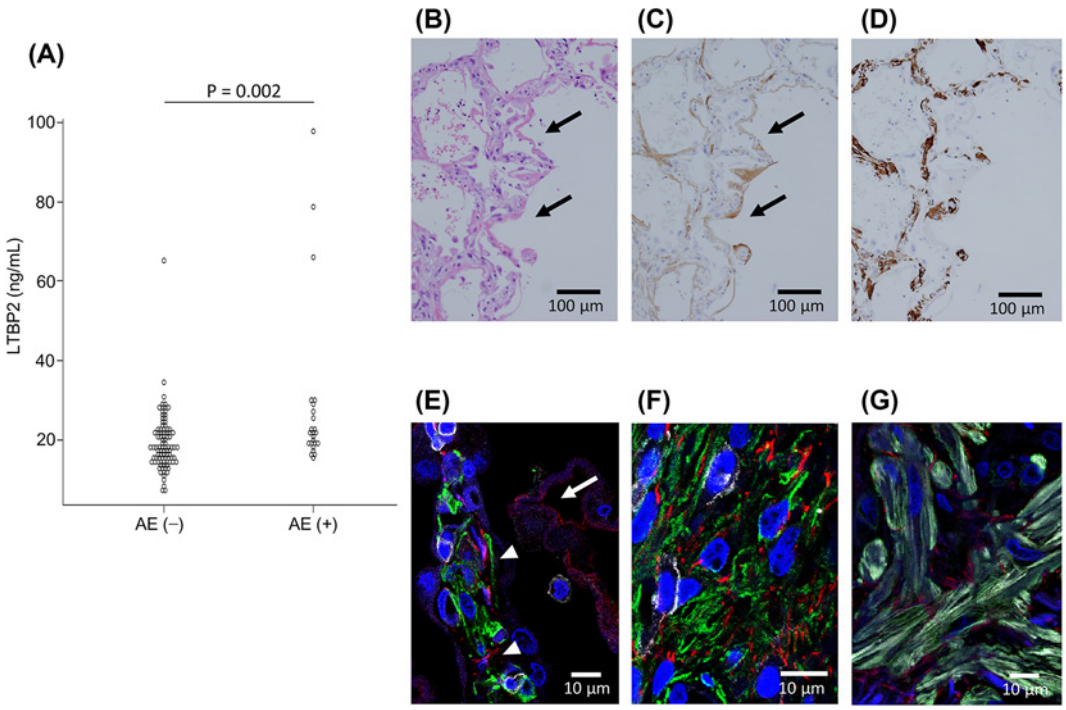

Figure 7. Association of LTBP2 with acute exacerbation (AE) of IPF

(**A**) Comparison of serum LTBP2 concentrations between patients with (*n*=24) and without (*n*=92) AE of IPF at IPF diagnosis or within 6 months of IPF diagnosis. Statistical comparison was performed using the Mann–Whitney U test. (**B**–**D**) Immunohistochemistry images of diffuse alveolar damage in an autopsied lung from a patient with AE of IPF, stained by Hematoxylin–Eosin, anti-LTBP2 antibody, and anti-αSMA antibody, respectively. Intra-alveolar LTBP2-positive hyaline membranes (arrows) and edematous alveolar walls with many αSMA-positive cells were observed. Hyaline membranes were not stained when a normal rabbit polyclonal IgG was used as the primary antibody. (**E**–**G**) Immunofluorescence images of the same lung section (color: green = αSMA; red = LTBP2; white = lineage markers (CD45, CD324, CD31, podoplanin, and h-caldesmon)). (E) LTBP2 positivity was found in or around interstitial myofibroblasts (triangles) and in the hyaline membrane (arrow). (F) In a thickened alveolar wall, diffuse positivity for both αSMA and LTBP2 was observed. (G) Smooth muscle cells (h-caldesmon-positive cells) at a fibrotic interstitium showed positivity for LTBP2 as well as αSMA.

hazard model analyses identified baseline PaO_2, % predicted FVC, % predicted DLCO, and serum LTBP2 concentrations as potential prognostic factors in patients with IPF (Table 3). The hazard ratios for an increase in serum LTBP2 concentration of 1 ng/ml were 1.038 for all-cause death (95% confidence interval: 1.024–1.053) and 1.040 for death by respiratory events (95% confidence interval: 1.026–1.054). The bootstrap method with 1000-fold replication estimated the mean hazard ratio commonly as 1.046 (S.D.: 0.014, minimum: 1.024, maximum: 1.138 for all-cause death; S.D.: 0.015, minimum: 1.024, maximum: 1.138 for death by respiratory events), which was comparable with the original value. Using time-dependent ROC curves, the ideal cut-off level for predicting a better/worse prognosis was calculated as 18 ng/ml (Figure 8). The ROC curves at the 60-month follow-up are shown in Supplementary Figure S4. Comparisons of clinical factors and survival curves based on this cut-off value are shown in Supplementary Table S5 and Figure 8, respectively.

Discussion

We identified *Ltbp2* as one of the several highly up-regulated genes in myofibroblasts by analyzing transcriptome data from freshly isolated steady-state fibroblasts and myofibroblasts from mouse lungs. The up-regulation of *Ltbp2* was reproduced in human lung myofibroblasts induced by TGF-β1. Importantly, the LTBP2 protein was excessively secreted from these differentiated cells *in vitro*. Serum concentrations of LTBP2 were associated with baseline % predicted FVC values, as well as the prognosis of patients with IPF, suggesting that serum LTBP2 is potentially a novel prognostic biomarker reflecting the level of differentiation of lung fibroblasts into myofibroblasts in patients with IPF.

Clinical Science (2018) **132** 1565–1580
https://doi.org/10.1042/CS20180435

Table 3 Analysis of prognostic factors in patients with IPF

	Death by all causes			Death by respiratory events		
	HR	**95% CI**	***P***	**HR**	**95% CI**	***P***
Age, years	1.031	0.995–1.068	NS	1.034	0.996–1.073	NS
Male	1.345	0.572–3.165	NS	1.243	0.526–2.941	NS
Current or former smoker	0.687	0.353–1.338	NS	0.618	0.315–1.215	NS
Smoking dose (pack-year)	0.995	0.986–1.003	NS	0.995	0.986–1.003	NS
PaO_2 on room air (Torr)	0.978	0.960–0.995	<0.05	0.980	0.962–0.999	<0.05
% predicted FVC (%)	0.970	0.956–0.985	<0.001	0.968	0.953–0.984	<0.001
% predicted DLCO (%)	0.978	0.957–0.999	<0.05	0.971	0.948–0.994	<0.05
Serum KL-6 (U/ml)	0.915	<1.000–>1.000	NS	1.000	<1.000–>1.000	NS
Serum SP-D (ng/ml)	1.001	<1.000–1.002	NS	1.001	<1.000–1.002	NS
Serum LDH (U/l)	1.002	0.998–1.006	NS	1.002	0.998–1.006	NS
Serum LTBP2 (ng/ml)	1.038	1.024–1.053	<0.001	1.040	1.026–1.054	<0.001

All *P*-values were evaluated by Cox's proportional hazard model. Abbreviations: CI, confidence interval; HR, hazard ratio; LDH, lactate dehydrogenase; NS, not significant; SP-D, surfactant protein-D.

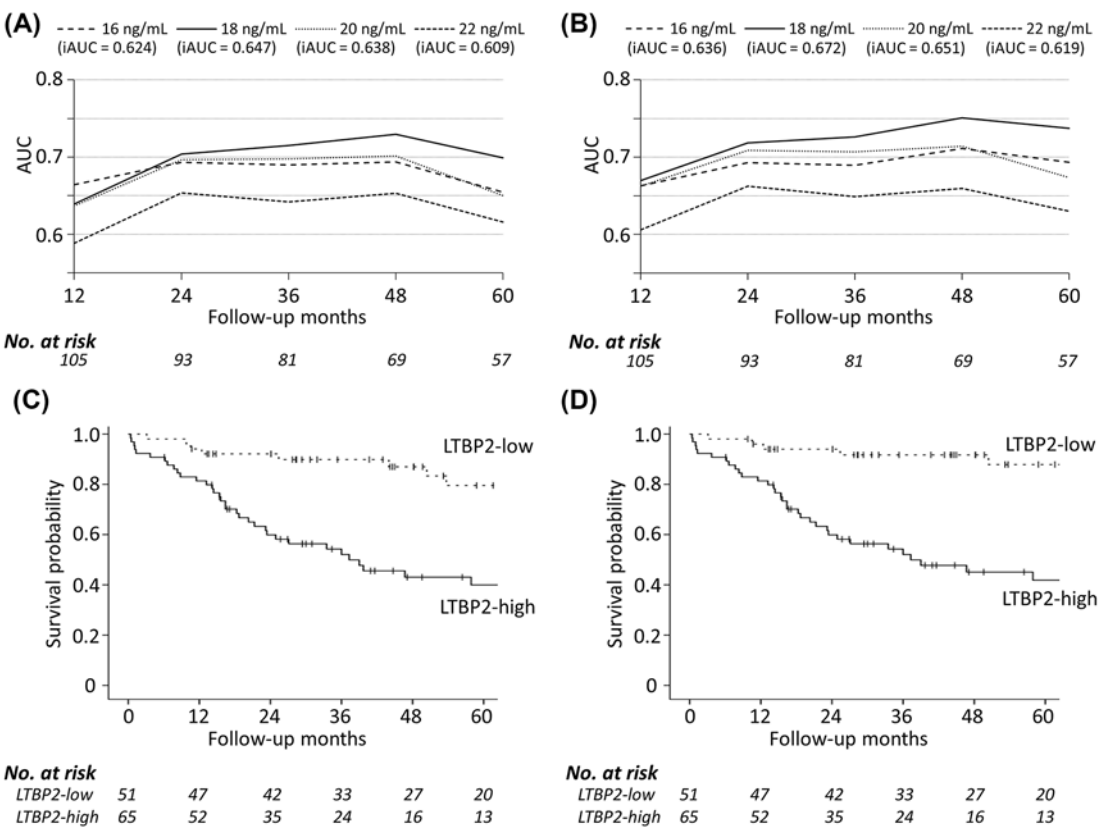

Figure 8. Prognostic analyses using serum LTBP2 concentrations

(**A**,**B**) Time-dependent ROC curves for all-cause death and death by respiratory events, respectively. Integrated AUC (iAUC) was calculated for each cut-off value of serum LTBP2 concentration. The cut-off value with the highest iAUC was estimated commonly as 18 ng/ml. (**C**,**D**) Survival curves drawn by the Kaplan–Meyer method using the cut-off value of 18 ng/ml for all-cause death and death by respiratory events, respectively. The prognostic difference was statistically significant ($P<0.001$ by log-rank test in both situations).

LTBP2, a fibrillin/LTBP superfamily protein, is an ECM protein with a molecular weight of 195–240 kDa. It is commonly expressed in the lungs, skin, and large vessels [26–28]. Although LTBP1, 3, and 4 can combine with latent TGF-β, only LTBP2 is present without combining; thus, the function of LTBP2 has not been fully clarified [28]. Although *Ltbp2*-knockout mice are reported to exhibit normal-structured lungs [29], a recent study demonstrated that a double knockout mouse lacking the *Ltbp2* and *Ltbp4S* genes exhibited a worsened emphysema compared with the single knockout mice lacking only *Ltbp4S* [30]. These data suggest a positive role of LTBP2 in lung elastinogenesis.

In addition to elastinogenesis, LTBP2 may be associated with fibrosis or tissue remodeling in several organs, including the skin, heart, and kidneys [31-33]; however, its biological role remains unknown. An *in vitro* study has revealed that LTBP2 competes with LTBP1 by binding to fibrillin-1, suggesting an indirect role of LTBP2 in the storage and activation of TGF-β, a major profibrotic growth factor [34]. In addition, Sideek et al. [35] recently reported that a bioactive region of LTBP2 can directly up-regulate TGF-β1 expression. On the other hand, previous studies suggested the antifibrotic role of LTBP2 via inhibition of fibroblast growth factor-2-induced fibroblast proliferation and fibroblast adhesion to fibronectin [36,37]. Therefore, future experiments using *Ltbp2*-knockout mice to assess lung fibrosis, as well as gene and/or protein analyses of isolated lung (myo)fibroblasts, may be necessary to determine the exact role of LTBP2 in fibrosis.

In the present study, up-regulation of LTBP2 at the mRNA and protein levels in human lung myofibroblasts induced by TGF-β1 was found. This is consistent with the results from a previous study that speculated the involvement of Ras or another related small GTP-binding protein in the signaling pathway [38]. In biopsied IPF lung sections, LTBP2 staining was almost negative in blood cells, epithelial cells, vascular endothelial cells, lymphatic endothelial cells, and (peribronchovascular and interstitial) smooth muscle cells, whereas the fibrotic interstitial space was broadly stained. Based on our immunofluorescence results, the majority of LTBP2 presented as an ECM protein; however, several non-aggregated (non-fibroblastic foci) myofibroblasts also stained positive for LTBP2, suggesting an origin of LTBP2 in fibrotic lungs. In contrast, as shown in Figure 7G, when a patient develops acute exacerbation of IPF, proliferated interstitial smooth muscle cells as well as non-fibroblastic foci myofibroblasts seem to be one of the sources of LTBP2. Collectively, during lung fibrosis, LTBP2 is produced by these abnormal mesenchymal cells and is secreted into the ECM where it likely colocalizes with several extracellular proteins, including elastin, fibrillin-1, and possibly other collagenous proteins, such as collagen and fibronectin [39,40]. In addition, some LTBP2 enters into blood vessels and can be detected as a serum protein.

To the best of our knowledge, no studies evaluating LTBP2 as a blood biomarker for IPF have been reported. Based on a previous proteome analysis using human plasma, higher LTBP2 concentrations were significantly associated with a worse prognosis, commonly due to pulmonary death, in patients who developed acute dyspnea [41]. The differentiation of lung fibroblasts into myofibroblasts is frequently observed, regardless of the underlying disease, when a patient develops acute respiratory distress syndrome or diffuse alveolar damage [42,43]. These findings may support our data showing that patients who developed acute exacerbation within 6 months of their IPF diagnosis, often with diffuse alveolar damage superimposed on the underlying UIP fibrosis [23], had significantly higher serum LTBP2 concentrations than those who did not. Moreover, although the mechanism is unclear, the LTBP2 positivity for hyaline membranes, in which various kinds of serum proteins are included [44], might also be a supportive evidence for the serum data of acute exacerbation. Taken together, LTBP2 as a biomarker can be used to evaluate not obsolete fibrosis but acute-phase and ongoing fibrogenesis. This leads to speculation that LTBP2-positive or -producing myofibroblasts are differentiating or newly differentiated cells compared with LTBP2-negative myofibroblasts configuring fibroblastic foci.

As previous researchers have indicated, serum LTBP2 concentrations can increase in several non-pulmonary diseases, such as cancer, heart failure, and renal dysfunction [14-22,32,45]. Additionally, in the present study, there was a considerable overlap of data in the serum LTBP2 concentrations between IPF patients and healthy subjects. These results imply that serum LTBP2 is insufficient as a 'diagnostic' biomarker for IPF. In order to improve the diagnostic accuracy, it may be worth considering combining LTBP2 with other existing markers like KL-6.

Our study has several limitations, particularly in the clinical aspect. First of all, this is a small single-cohort retrospective study. To validate our preliminary results, a future large-scale, multi-cohort prospective study is warranted. In addition, we could not evaluate the chronological changes of serum LTBP2 concentrations in the same IPF patients. Perhaps, such changes might be more important than the one-point value itself, which may explain why several patients showed relatively low serum LTBP2 concentrations even during the acute exacerbation of IPF. Moreover, to clarify the utility of LTBP2, it is necessary to study the serum concentrations in patients with other pulmonary diseases including infectious pneumonias, bronchial asthma, and particularly interstitial lung diseases except IPF. These can be future research topics.

Clinical Science (2018) **132** 1565–1580
https://doi.org/10.1042/CS20180435

Within these limitations, in conclusion, we demonstrated that serum LTBP2, which may correspond to TGF-β1-induced differentiation of lung fibroblasts into myofibroblasts, is a potential prognostic biomarker for IPF.

Clinical perspectives

- IPF is a chronic, progressive, fibrotic lung disease with high mortality. Although differentiation of lung fibroblasts into myofibroblasts is known to be important in disease progression, few biomarkers reflecting the fibrotic process have been discovered.
- Our transcriptome analysis identified *Ltbp2*, the gene encoding LTBP2, as a significantly up-regulated gene in myofibroblasts isolated from bleomycin-treated mouse lungs using FACS. This up-regulation was reproduced at the mRNA and protein levels in human lung myofibroblasts induced by TGF-β1. Intriguingly, serum LTBP2 concentrations in IPF patients were higher than those in healthy volunteers and the increase was significantly associated with a worse prognosis.
- Serum LTBP2, which may correspond to TGF-β1-induced differentiation of lung fibroblasts into myofibroblasts, is a potential prognostic biomarker in patients with IPF.

Acknowledgements
We thank all staff of Department of Regenerative and Infectious Pathology, Hamamatsu University School of Medicine (Mr Kaneta, Ms Suzuki, Ms Kawashima, and Ms Muranaka) for their technical assistance. We also thank all staff of Second Division, Department of Internal Medicine, Hamamatsu University School of Medicine, particularly Dr Furuhashi, Dr Suzuki, Dr Karayama, Dr Hozumi, Dr Kono, Dr Yasui, Dr Oyama, Dr Yoshimura, Dr Nishimoto, Dr Akiyama, Ms Oishi, Ms Takeuchi, and Ms Onaka for their data acquisition. We appreciate the statistical advice from Dr Yamakage (SATISTA Inc., Japan).

Competing interests
The authors declare that there are no competing interests associated with the manuscript.

Funding
This work was supported by grant-in-aid for Scientific Research (C) from the Japan Society for the Promotion of Science [grant number 16K08736].

Author contribution
Y.E. and T.I. designed the study. Y.E., S.Matsushima, K.S., Y.A., H.Y., S.Meguro, H.K., I.K., T.F., N.E., N.I., Y.N., and T.S. collected data. All authors contributed to data interpretation. Y.E. and T.I. wrote the original manuscript. All authors contributed to the revisions of the manuscript, and agreed to be accountable for all aspects of the work.

Abbreviations
αSMA, α-smooth muscle actin; AUC, area under curve; C_T, cycle threshold; DLCO, diffusion capacity for carbon monoxide; ECM, extracellular matrix; FVC, forced vital capacity; IPF, idiopathic pulmonary fibrosis; KL-6, Krebs von den Lungen-6; LTBP2, latent transforming growth factor-β binding protein-2; qRT-PCR, quantitative reverse transcription-PCR; ROC, receiver operating characteristic; RT-PCR, reverse transcription-PCR; TGF-β, transforming growth factor-β; UIP, usual interstitial pneumonia.

References
1 Raghu, G., Collard, H.R., Egan, J.J., Martinez, F.J., Behr, J., Brown, K.K. et al. (2011) An official ATS/ERS/JRS/ALAT statement: idiopathic pulmonary fibrosis: evidence-based guidelines for diagnosis and management. *Am. J. Respir. Crit. Care Med.* **183**, 788–824, https://doi.org/10.1164/rccm.2009-040GL
2 Blackwell, T.S., Tager, A.M., Borok, Z., Moore, B.B., Schwartz, D.A., Anstrom, K.J. et al. (2014) Future directions in idiopathic pulmonary fibrosis research. An NHLBI workshop report. *Am. J. Respir. Crit. Care Med.* **189**, 214–222, https://doi.org/10.1164/rccm.201306-1141WS
3 Pardo, A. and Selman, M. (2016) Lung fibroblasts, aging, and idiopathic pulmonary fibrosis. *Ann. Am. Thorac. Soc.* **13** (Supplement 5), S417–S421, https://doi.org/10.1513/AnnalsATS.201605-341AW
4 Mackinnon, A.C., Gibbons, M.A., Farnworth, S.L., Leffler, H., Nilsson, U.J., Delaine, T. et al. (2012) Regulation of transforming growth factor-β1–driven lung fibrosis by galectin-3. *Am. J. Respir. Crit. Care Med.* **185**, 537–546, https://doi.org/10.1164/rccm.201106-09650C

5 Hu, B., Wu, Z. and Phan, S.H. (2003) Smad3 mediates transforming growth factor-beta-induced alpha-smooth muscle actin expression. *Am. J. Respir. Cell Mol. Biol.* **29**, 397–404, https://doi.org/10.1165/rcmb.2003-0063OC
6 Guo, W., Shan, B., Klingsberg, R.C., Qin, X. and Lasky, J.A. (2009) Abrogation of TGF-beta 1-induced fibroblast-myofibroblast differentiation by histone deacetylase inhibition. *Am. J. Physiol. Lung Cell Mol. Physiol.* **297**, L864–L870, https://doi.org/10.1152/ajplung.00128.2009
7 Ley, B., Ryerson, C.J., Vittinghoff, E., Ryu, J.H., Tomassetti, S., Lee, J.S. et al. (2012) A multidimensional index and staging system for idiopathic pulmonary fibrosis. *Ann. Intern. Med.* **156**, 684–691, https://doi.org/10.7326/0003-4819-156-10-201205150-00004
8 Rosas, I.O., Richards, T.J., Konishi, K., Zhang, Y., Gibson, K., Lokshin, A.E. et al. (2008) MMP1 and MMP7 as potential peripheral blood biomarkers in idiopathic pulmonary fibrosis. *PLoS Med.* **5**, e93, https://doi.org/10.1371/journal.pmed.0050093
9 Vij, R. and Noth, I. (2012) Peripheral blood biomarkers in idiopathic pulmonary fibrosis. *Transl. Res.* **159**, 218–227, https://doi.org/10.1016/j.trsl.2012.01.012
10 Vuga, L.J., Tedrow, J.R., Pandit, K.V., Tan, J., Kass, D.J., Xue, J. et al. (2014) C-X-C motif chemokine 13 (CXCL13) is a prognostic biomarker of idiopathic pulmonary fibrosis. *Am. J. Respir. Crit. Care Med.* **189**, 966–974, https://doi.org/10.1164/rccm.201309-1592OC
11 White, E.S., Xia, M., Murray, S., Dyal, R., Flaherty, C.M., Flaherty, K.R. et al. (2016) Plasma surfactant protein-D, matrix metalloproteinase-7, and osteopontin index distinguishes idiopathic pulmonary fibrosis from other idiopathic interstitial pneumonias. *Am. J. Respir. Crit. Care Med.* **194**, 1242–1251, https://doi.org/10.1164/rccm.201505-0862OC
12 Akamatsu, T., Arai, Y., Kosugi, I., Kawasaki, H., Meguro, S., Sakao, M. et al. (2013) Direct isolation of myofibroblasts and fibroblasts from bleomycin-injured lungs reveals their functional similarities and differences. *Fibrogenesis Tissue Repair* **6**, 15, https://doi.org/10.1186/1755-1536-6-15
13 Richeldi, L., du Bois, R.M., Raghu, G., Azuma, A., Brown, K.K., Costabel, U. et al. (2014) Efficacy and safety of nintedanib in idiopathic pulmonary fibrosis. *N. Engl. J. Med.* **370**, 2071–2082, https://doi.org/10.1056/NEJMoa1402584
14 da Costa, A.N., Plymoth, A., Santos-Silva, D., Ortiz-Cuaran, S., Camey, S., Guilloreau, P. et al. (2015) Osteopontin and latent-TGF β binding-protein 2 as potential diagnostic markers for HBV-related hepatocellular carcinoma. *Int. J. Cancer* **136**, 172–181, https://doi.org/10.1002/ijc.28953
15 Wan, F., Peng, L., Zhu, C., Zhang, X., Chen, F. and Liu, T. (2017) Knockdown of latent transforming growth factor-β (TGF-β)-binding protein 2 (LTBP2) inhibits invasion and tumorigenesis in thyroid carcinoma cells. *Oncol. Res.* **25**, 503–510, https://doi.org/10.3727/096504016X14755368915591
16 Torres, S., Bartolomé, R.A., Mendes, M., Barderas, R., Fernandez-Aceñero, M.J., Peláez-García, A. et al. (2013) Proteome profiling of cancer-associated fibroblasts identifies novel proinflammatory signatures and prognostic markers for colorectal cancer. *Clin. Cancer Res.* **19**, 6006–6019, https://doi.org/10.1158/1078-0432.CCR-13-1130
17 Chan, S.H.K., Yee Ko, J.M., Chan, K.W., Chan, Y.P., Tao, Q., Hyytiainen, M. et al. (2011) The ECM protein LTBP-2 is a suppressor of esophageal squamous cell carcinoma tumor formation but higher tumor expression associates with poor patient outcome. *Int. J. Cancer* **129**, 565–573, https://doi.org/10.1002/ijc.25698
18 Turtoi, A., Musmeci, D., Wang, Y., Dumont, B., Somja, J., Bevilacqua, G. et al. (2011) Identification of novel accessible proteins bearing diagnostic and therapeutic potential in human pancreatic ductal adenocarcinoma. *J. Proteome Res.* **10**, 4302–4313, https://doi.org/10.1021/pr200527z
19 Yoshihara, K., Tajima, A., Komata, D., Yamamoto, T., Kodama, S., Fujiwara, H. et al. (2009) Gene expression profiling of advanced-stage serous ovarian cancers distinguishes novel subclasses and implicates ZEB2 in tumor progression and prognosis. *Cancer Sci.* **100**, 1421–1428, https://doi.org/10.1111/j.1349-7006.2009.01204.x
20 Han, L., Tang, M.M., Xu, X., Jiang, B., Huang, J., Feng, X. et al. (2016) LTBP2 is a prognostic marker in head and neck squamous cell carcinoma. *Oncotarget* **7**, 45052–45059
21 Ren, Y., Lu, H., Zhao, D., Ou, Y., Yu, K., Gu, J. et al. (2015) LTPB2 acts as a prognostic factor and promotes progression of cervical adenocarcinoma. *Am. J. Transl. Res.* **7**, 1095–1105
22 Chang, J., Xu, W., Liu, G., Du, X. and Li, X. (2017) Down-regulation of LTBP2 suppresses the proliferation, migration and invasion in human prostate cancer cells. *Int. J. Clin. Exp. Pathol.* **10**, 6759–6766
23 Collard, H.R., Ryerson, C.J., Corte, T.J., Jenkins, G., Kondoh, Y., Lederer, D.J. et al. (2016) Acute exacerbation of idiopathic pulmonary fibrosis. an international working group report. *Am. J. Respir. Crit. Care Med.* **194**, 265–275, https://doi.org/10.1164/rccm.201604-0801CI
24 Efron, B. and Tibshirani, R. (1993) *An Introduction to the Bootstrap*, Chapman and Hall, New York
25 Heagerty, P.J. and Zheng, Y. (2005) Survival model predictive accuracy and ROC curves. *Biometrics* **61**, 92–105, https://doi.org/10.1111/j.0006-341X.2005.030814.x
26 Morén, A., Olofsson, A., Stenman, G., Sahlin, P., Kanzaki, T., Claesson-Welsh, L. et al. (1994) Identification and characterization of LTBP-2, a novel latent transforming growth factor-beta-binding protein. *J. Biol. Chem.* **269**, 32469–32478
27 Shipley, J.M., Mecham, R.P., Maus, E., Bonadio, J., Rosenbloom, J., McCarthy, R.T. et al. (2000) Developmental expression of latent transforming growth factor beta binding protein 2 and its requirement early in mouse development. *Mol. Cell. Biol.* **20**, 4879–4887, https://doi.org/10.1128/MCB.20.13.4879-4887.2000
28 Gibson, M.A., Hatzinikolas, G., Davis, E.C., Baker, E., Sutherland, G.R. and Mecham, R.P. (1995) Bovine latent transforming growth factor beta 1-binding protein 2: molecular cloning, identification of tissue isoforms, and immunolocalization to elastin-associated microfibrils. *Mol. Cell. Biol.* **15**, 6932–6942, https://doi.org/10.1128/MCB.15.12.6932
29 Inoue, T., Ohbayashi, T., Fujikawa, Y., Yoshida, H., Akama, T.O., Noda, K. et al. (2014) Latent TGF-β binding protein-2 is essential for the development of ciliary zonule microfibrils. *Hum. Mol. Genet.* **23**, 5672–5682, https://doi.org/10.1093/hmg/ddu283
30 Fujikawa, Y., Yoshida, H., Inoue, T., Ohbayashi, T., Noda, K., von Melchner, H. et al. (2017) Latent TGF-β binding protein 2 and 4 have essential overlapping functions in microfibril development. *Sci. Rep.* **7**, 43714, https://doi.org/10.1038/srep43714
31 Sideek, M.A., Teia, A., Kopecki, Z., Cowin, A.J. and Gibson, M.A. (2016) Co-localization of LTBP-2 with FGF-2 in fibrotic human keloid and hypertrophic scar. *J. Mol. Histol.* **47**, 35–45, https://doi.org/10.1007/s10735-015-9645-0

Clinical Science (2018) **132** 1565–1580
https://doi.org/10.1042/CS20180435

32 Bai, Y., Zhang, P., Zhang, X., Huang, J., Hu, S. and Wei, Y. (2012) LTBP-2 acts as a novel marker in human heart failure - a preliminary study. *Biomarkers* **17**, 407–415, https://doi.org/10.3109/1354750X.2012.677860
33 Kim, Y.S., Kang, H.S., Herbert, R., Beak, J.Y., Collins, J.B., Grissom, S.F. et al. (2008) Kruppel-like zinc finger protein Glis2 is essential for the maintenance of normal renal functions. *Mol. Cell Biol.* **28**, 2358–2367, https://doi.org/10.1128/MCB.01722-07
34 Hirani, R., Hanssen, E. and Gibson, M.A. (2007) LTBP-2 specifically interacts with the amino-terminal region of fibrillin-1 and competes with LTBP-1 for binding to this microfibrillar protein. *Matrix Biol.* **26**, 213–223, https://doi.org/10.1016/j.matbio.2006.12.006
35 Sideek, M.A., Smith, J., Menz, C., Adams, J.R.J., Cowin, A.J. and Gibson, M.A. (2017) A central bioactive region of LTBP-2 stimulates the expression of TGF-β1 in fibroblasts via Akt and p38 signalling pathways. *Int. J. Mol. Sci.* **18**, E2114, https://doi.org/10.3390/ijms18102114
36 Menz, C., Parsi, M.K., Adams, J.R., Sideek, M.A., Kopecki, Z., Cowin, A.J. et al. (2015) LTBP-2 has a single high-affinity binding site for FGF-2 and blocks FGF-2-induced cell proliferation. *PLoS ONE* **10**, e0135577, https://doi.org/10.1371/journal.pone.0135577
37 Hyytiäinen, M. and Keski-Oja, J. (2003) Latent TGF-beta binding protein LTBP-2 decreases fibroblast adhesion to fibronectin. *J. Cell Biol.* **163**, 1363–1374, https://doi.org/10.1083/jcb.200309105
38 Ahmed, W., Kucich, U., Abrams, W., Bashir, M., Rosenbloom, J., Segade, F. et al. (1998) Signaling pathway by which TGF-beta1 increases expression of latent TGF-beta binding protein-2 at the transcriptional level. *Connect. Tissue Res.* **37**, 263–276, https://doi.org/10.3109/03008209809002444
39 Vehviläinen, P., Hyytiäinen, M. and Keski-Oja, J. (2009) Matrix association of latent TGF-beta binding protein-2 (LTBP-2) is dependent on fibrillin-1. *J. Cell. Physiol.* **221**, 586–593, https://doi.org/10.1002/jcp.21888
40 Mangasser-Stephan, K., Gartung, C., Lahme, B. and Gressner, A.M. (2001) Expression of isoforms and splice variants of the latent transforming growth factor beta binding protein (LTBP) in cultured human liver myofibroblasts. *Liver* **21**, 105–113, https://doi.org/10.1034/j.1600-0676.2001.021002105.x
41 Breidthardt, T., Vanpoucke, G., Potocki, M., Mosimann, T., Ziller, R., Thomas, G. et al. (2012) The novel marker LTBP2 predicts all-cause and pulmonary death in patients with acute dyspnoea. *Clin. Sci. (Lond.)* **123**, 557–566, https://doi.org/10.1042/CS20120058
42 Pache, J.C., Christakos, P.G., Gannon, D.E., Mitchell, J.J., Low, R.B. and Leslie, K.O. (1998) Myofibroblasts in diffuse alveolar damage of the lung. *Mod. Pathol.* **11**, 1064–1070
43 Thille, A.W., Esteban, A., Fernández-Segoviano, P., Rodriguez, J.M., Aramburu, J.A., Vargas-Errázuriz, P. et al. (2013) Chronology of histological lesions in acute respiratory distress syndrome with diffuse alveolar damage: a prospective cohort study of clinical autopsies. *Lancet Respir. Med.* **1**, 395–401, https://doi.org/10.1016/S2213-2600(13)70053-5
44 Sun, A.P., Ohtsuki, Y., Fujita, J., Ishida, T., Yoshinouchi, T. and Kohno, N. (2003) Immunohistochemical characterisation of pulmonary hyaline membrane in various types of interstitial pneumonia. *Pathology* **35**, 120–124
45 Haase, M., Bellomo, R., Albert, C., Vanpoucke, G., Thomas, G., Laroy, W. et al. (2014) The identification of three novel biomarkers of major adverse kidney events. *Biomark. Med.* **8**, 1207–1217, https://doi.org/10.2217/bmm.14.90

Supplementary material

Title:

LTBP2 is secreted from lung myofibroblasts and is a potential biomarker for idiopathic pulmonary fibrosis

Authors:

Yasunori Enomoto, Sayomi Matsushima, Kiyoshi Shibata, Yoichiro Aoshima, Haruna Yagi, Shiori Meguro, Hideya Kawasaki, Isao Kosugi, Tomoyuki Fujisawa, Noriyuki Enomoto, Naoki Inui, Yutaro Nakamura, Takafumi Suda, Toshihide Iwashita

Supplementary Tables

Table S1. Antibodies used in FACS

Primary antibody	Target cells	Fluorescence	Company	Dilution
Anti-CD45	Blood cells	APC	BioLegend	1:150
Anti-TER-119	Erythrocytes	APC	eBioscience	1:150
Anti-CD324 (E-cadherin)	Epithelial cells	APC	BioLegend	1:150
Anti-CD31	Vascular endothelial cells	APC	BioLegend	1:150
Anti-CD146	Smooth muscle cells and pericytes	APC	BioLegend	1:150
Anti-LYVE1	Lymphatic endothelial cells	APC	R&D	1:60
Anti-Sca-1	Fibroblasts	PE-Cy7	eBioscience	1:600
Anti-PDGFRα (CD140a)	Fibroblasts	PE	BioLegend	1:50
Streptavidin	(Biotin)	PerCP-Cy5.5	BioLegend	1:300
Anti-CD49e (integrin	Myofibroblasts (cell surface	(Biotin)	Abcam	1:150

α5)	marker)			
Anti-α-smooth muscle actin	Myofibroblasts (intra-cellular protein)	FITC	Abcam	1:100

Table S2. Genes that are highly upregulated in myofibroblasts (MFB) or steady-state fibroblasts (FB) from mouse lungs

Genes upregulated in MFB	**Symbol**	**MFB-signal**	**FB-signal**	**Fold change (MFB/FB)**
Secreted phosphoprotein 1	*Spp1*	156374.3	15.1	10351.5
Gremlin 1	*Grem1*	16794.8	14.6	1153.1
Kinesin family member 26B	*Kif26b*	17524.0	17.8	984.3
Thrombospondin 4	*Thbs4*	79551.2	164.4	483.8
Collagen triple helix repeat containing 1	*Cthrc1*	32474.7	141.2	230.0
Periostin, osteoblast specific factor	*Postn*	49741.5	224.0	222.0
Tenascin C	*Tnc*	35515.7	186.9	190.0
Chondrolectin	*Chodl*	17701.0	105.8	167.4
Desmin	*Des*	43449.3	442.6	98.2
Inhibin beta-A	*Inhba*	93682.0	1789.1	52.4
Collagen, type VIII, alpha 1	*Col8a1*	12495.5	262.7	47.6
Baculoviral IAP repeat-containing 5	*Birc5*	43879.4	1225.4	35.8
Actin, alpha 2, smooth muscle, aorta	*Acta2*	106982.3	3203.1	33.4
SHC (Src homology 2 domain containing) family, member 4	*Shc4*	29557.0	937.9	31.5
Scleraxis	*Scx*	19402.9	656.0	29.6
Heparin-binding EGF-like growth factor	*Hbegf*	25328.7	887.9	28.5
Procollagen-proline, 2-oxoglutarate 4-dioxygenase	*P4ha3*	48170.5	1712.9	28.1
Transforming, acidic coiled-coil containing protein 3	*Tacc3*	12922.9	495.0	26.1
Latent transforming growth factor beta binding protein 2	*Ltbp2*	112347.8	4430.0	25.4
Activity regulated cytoskeletal-associated protein	*Arc*	14632.2	686.5	21.3
Mesenchyme homeobox 1	*Meox1*	15498.8	727.3	21.3

Actin, gamma 2, smooth muscle, enteric	*Actg2*	22188.7	1146.0	19.4
Pleiotrophin	*Ptn*	17711.5	930.7	19.0
Zinc finger, DHHC domain containing 3	*Zdhhc3*	28057.0	1683.2	16.7
Collagen, type VII, alpha 1	*Col7a1*	38948.6	2678.5	14.5
2,3-bisphosphoglycerate mutase	*Bpgm*	111491.4	7866.0	14.2
Collagen, type XII, alpha 1	*Col12a1*	150876.1	12420.8	12.1
Family with sequence similarity 173, member B	*Fam173b*	14059.1	1162.7	12.1
Neuronal regeneration related protein	*Nrep*	90753.0	7789.2	11.7
Tissue inhibitor of metalloproteinase 1	*Timp1*	51218.5	4468.9	11.5
Discs, large (Drosophila) homolog-associated protein 2	*Dlgap2*	12334.5	1111.7	11.1
Fibronectin 1	*Fn1*	108667.5	10496.6	10.4
Transgelin	*Tagln*	99265.9	9621.9	10.3
Collagen, type V, alpha 3	*Col5a3*	25504.9	2504.9	10.2
Tropomyosin 2, beta	*Tpm2*	117555.4	12240.7	9.6
Lysyl oxidase-like 2	*Loxl2*	27945.0	3375.2	8.3
Elastin	*Eln*	375373.3	48597.3	7.7
Collagen, type V, alpha 1	*Col5a1*	97043.5	15209.0	6.4
Sarcosine dehydrogenase	*Sardh*	13725.2	2195.3	6.3
Collagen, type IV, alpha 2	*Col4a2*	29962.5	4908.1	6.1
Chemokine (C-C motif) ligand 2	*Ccl2*	12963.0	2201.0	5.9
SPEG complex locus	*Speg*	17501.8	2999.8	5.8
Collagen, type VI, alpha 3	*Col6a3*	16958.0	3189.0	5.3
Secreted acidic cysteine rich glycoprotein	*Sparc*	554817.5	105624.7	5.3
Genes upregulated in steady-state FB	**Symbol**	**MFB-signal**	**FB-signal**	**Fold change (FB/MFB)**
Delta/notch-like EGF-related receptor	*Dner*	319.6	15308.1	47.9
Sodium channel, voltage-gated, type III, alpha	*Scn3a*	425.7	14025.8	32.9
ABI gene family, member 3 (NESH) binding protein	*Abi3bp*	465.9	13804.5	29.6
FMS-like tyrosine kinase 3 ligand	*Flt3l*	2997.3	88458.0	29.5
Retinol binding protein 4, plasma	*Rbp4*	569.2	16108.8	28.3
Solute carrier family 10 (sodium/bile acid cotransporter family), member 6	*Slc10a6*	763.1	16598.2	21.8
Gamma-aminobutyric acid (GABA) A receptor, subunit alpha 3	*Gabra3*	2820.6	50110.7	17.8
Adrenergic receptor, beta 3	*Adrb3*	800.3	13909.5	17.4
Epidermal growth factor-containing fibulin-like extracellular matrix protein 1	*Efemp1*	4169.3	71505.8	17.2
Cell adhesion molecule-related/down-regulated by oncogenes	*Cdon*	1643.3	27186.1	16.5
Mitochondrial transcription termination factor 4	*Mterf4*	1376.0	21849.2	15.9

Dipeptidase 1 (renal)	*Dpep1*	3009.2	47483.6	15.8
ATP-binding cassette, sub-family A (ABC1), member 8a	*Abca8a*	1325.0	19997.0	15.1
Fibulin 1	*Fbln1*	7692.5	108968.4	14.2
Apolipoprotein D	*Apod*	2072.4	29043.0	14.0
Phosphatidic acid phosphatase type 2B	*Ppap2b*	3124.7	43473.8	13.9
A kinase (PRKA) anchor protein (gravin) 12	*Akap12*	10163.1	136662.8	13.4
Growth differentiation factor 10	*Gdf10*	4296.0	56210.1	13.1
Complement component 7	*C7*	1347.9	16344.2	12.1
Complement component factor h	*Cfh*	9081.6	108051.4	11.9
Osteoglycin	*Ogn*	5302.9	62204.3	11.7
Solute carrier family 38, member 5	*Slc38a5*	5386.2	59901.3	11.1
Matrix metallopeptidase 3	*Mmp3*	3321.7	34777.3	10.5
RGD motif, leucine rich repeats, tropomodulin domain and proline-rich containing	*Rltpr*	1911.5	19913.5	10.4
Coagulation factor III	*F3*	4354.1	43716.7	10.0
Progestin and adipoQ receptor family member VI	*Paqr6*	1668.1	16197.0	9.7
Hedgehog-interacting protein	*Hhip*	1388.7	13304.8	9.6
Complement factor H-related 2	*Cfhr2*	4355.1	40274.9	9.2
3-hydroxy-3-methylglutaryl-Coenzyme A synthase 2	*Hmgcs2*	2037.9	18390.0	9.0
Gelsolin	*Gsn*	72027.0	647052.8	9.0
Bone morphogenetic protein 4	*Bmp4*	3748.1	33637.8	9.0
Hydroxysteroid 11-beta dehydrogenase 1	*Hsd11b1*	4025.1	35932.1	8.9
Podocan	*Podn*	1918.9	16890.0	8.8
Glypican 6	*Gpc6*	2993.9	24704.9	8.3
Integrin, beta-like 1	*Itgbl1*	1918.1	15445.6	8.1
Angiopoietin 1	*Angpt1*	4720.3	36485.2	7.7
Platelet derived growth factor receptor, alpha polypeptide	*Pdgfra*	11852.0	86126.0	7.3
Insulin-like growth factor binding protein 6	*Igfbp6*	8787.8	63348.0	7.2
Complement component 4B (Chido blood group)	*C4b*	6995.2	49948.4	7.1
Very low density lipoprotein receptor	*Vldlr*	2062.4	14483.7	7.0
C-fos induced growth factor	*Figf*	4176.8	28956.9	6.9
Sulfotransferase family 5A, member 1	*Sult5a1*	7031.9	48640.0	6.9
Complement component 1, s subcomponent 2	*C1s2*	9771.5	66757.1	6.8
Decorin	*Dcn*	24793.5	167281.3	6.7
Integrin alpha 8	*Itga8*	8519.4	56961.3	6.7
Neuroblastoma, suppression of tumorigenicity 1	*Nbl1*	7885.3	52238.2	6.6

Peptidase inhibitor 16	*Pi16*	2352.5	14502.6	6.2
Tumor necrosis factor alpha induced protein 6	*Tnfaip6*	6374.6	38703.5	6.1
HtrA serine peptidase 3	*Htra3*	5375.2	31504.5	5.9
Complement component 3	*C3*	62397.1	363510.2	5.8
Complement component 1, s subcomponent 1	*C1s1*	9683.9	56265.3	5.8
Collagen, type XIII, alpha 1	*Col13a1*	5510.2	31843.6	5.8
Alcohol dehydrogenase 1 (class I)	*Adh1*	14653.7	79543.6	5.4
Sushi, von Willebrand factor type A, EGF and pentraxin domain containing 1	*Svep1*	8957.6	47882.3	5.3
Interleukin 6	*Il6*	6277.5	33302.5	5.3
NADPH oxidase 4	*Nox4*	4753.6	24154.9	5.1
Sema domain, immunoglobulin domain (Ig), short basic domain, secreted, (semaphorin) 3D	*Sema3d*	2641.6	13387.7	5.1
Slit homolog 3 (Drosophila)	*Slit3*	7279.1	36823.0	5.1
RNA binding motif, single stranded interacting protein	*Rbms3*	2767.8	13864.8	5.0

Genes that are upregulated in MFB were selected according to the following criteria: (1) five-fold greater than in steady-state FB; (2) five-fold greater than in total lung homogenates; and (3) two-fold greater than the mean value of all genes in MFB. Conversely, genes upregulated in steady-state FB were defined according to the following criteria: (1) five-fold greater than in MFB; (2) five-fold greater than in total lung homogenates; and (3) two-fold greater than the mean value of all genes in steady-state FB. The listed genes are available in the NCBI Reference Sequence.

Table S3. Gene ontology profiles of genes that are highly upregulated in myofibroblasts (MFB) or steady-state fibroblasts (FB) from mouse lungs

Gene ontology terms of upregulated genes in MFB	Number (n = 44)	p
Proteinaceous extracellular matrix	17	5.60E-18
Extracellular matrix	15	1.40E-17
Basement membrane	11	1.50E-14
Secreted	22	1.10E-12
Extracellular space	20	2.00E-10
Extracellular region	21	3.20E-10
Collagen	8	3.30E-10
Endodermal cell differentiation	6	4.60E-09
ECM-receptor interaction	8	8.00E-09
Collagen triple helix repeat	7	1.10E-08
Hydroxylation	7	2.10E-08
Signal peptide	25	2.40E-08
Signal	27	2.80E-08
Collagen trimer	7	3.40E-08
Focal adhesion	9	1.70E-07
Protein digestion and absorption	7	2.70E-07
Domain:Fibronectin type-III 9	4	7.40E-06
Disulfide bond	19	1.30E-05
Cell adhesion	9	1.60E-05
Domain:Fibronectin type-III 7	4	3.00E-05
TSPN	4	3.90E-05
Short sequence motif:Cell attachment site	5	4.10E-05
Domain:Fibronectin type-III 6	4	4.80E-05
Glycoprotein	20	5.20E-05
Fibronectin, type III	6	7.60E-05
Region of interest:Nonhelical region (NC2)	3	8.70E-05
PI3K-Akt signaling pathway	8	8.90E-05
Domain:Fibronectin type-III 14	3	1.20E-04
Extracellular matrix structural constituent	4	1.20E-04
Region of interest:Nonhelical region (NC1)	3	1.20E-04
Domain:Fibronectin type-III 5	4	1.30E-04
Extracellular matrix organization	5	1.50E-04
Domain:Fibronectin type-III 2	5	2.30E-04
Domain:Fibronectin type-III 1	5	2.40E-04
Laminin G domain	4	2.40E-04
Domain:Fibronectin type-III 11	3	2.60E-04
Domain:Fibronectin type-III 12	3	2.60E-04
Domain:Fibronectin type-III 10	3	3.20E-04
Domain:Fibronectin type-III 4	4	3.80E-04
Domain:Fibronectin type-III 3	4	8.40E-04
Region of interest:Triple-helical region	3	8.70E-04
Domain:TSP N-terminal	3	9.70E-04
Gene ontology terms of upregulated genes in steady-state FB	**Number (n = 59)**	**p**

Disulfide bond	40	3.20E-20
Signal peptide	41	6.10E-19
Signal	44	2.50E-18
Extracellular region	31	3.00E-17
Disulfide bond	36	5.40E-17
Extracellular space	29	6.80E-17
Secreted	29	1.00E-16
EGF-like domain	10	6.20E-09
EGF-like calcium-binding, conserved site	8	1.20E-08
EGF-type aspartate/asparagine hydroxylation site	8	1.20E-08
EGF-like calcium-binding	8	7.10E-08
Insulin-like growth factor binding protein, N-terminal	8	8.80E-08
Complement activation	5	1.10E-07
Proteinaceous extracellular matrix	10	2.90E-07
Complement and coagulation cascades	7	3.00E-07
EGF_CA	8	5.10E-07
Sushi/SCR/CCP	6	5.50E-07
Anaphylatoxin/fibulin	4	7.80E-07
Classical Complement Pathway	5	1.40E-06
CCP	6	2.00E-06
ANATO	4	2.00E-06
Blood microparticle	7	2.30E-06
Epidermal growth factor-like domain	8	5.00E-06
EGF	8	5.80E-06
Complement Pathway	5	8.30E-06
Growth factor	6	2.00E-05
EGF-like, conserved site	7	2.10E-05
Domain:EGF-like 1	6	2.40E-05
Staphylococcus aureus infection	5	3.30E-05
Extracellular matrix	7	3.30E-05
Domain:Anaphylatoxin-like	3	5.70E-05
Complement C3a/C4a/C5a anaphylatoxin	3	8.00E-05
Anaphylatoxin	3	8.00E-05
Lectin Induced Complement Pathway	4	9.80E-05
Growth factor activity	6	1.00E-04
Pertussis	5	1.50E-04
Domain:Sushi 1	4	1.70E-04
Domain:Sushi 2	4	1.70E-04
Sushi	4	2.50E-04
Positive regulation of ERK1 and ERK2 cascade	6	2.90E-04
Cross-link:Isoglutamyl cysteine thioester (Cys-Gln)	3	3.40E-04
Calcium ion binding	10	3.50E-04
Alpha-2-macroglobulin, conserved site	3	3.60E-04
Alpha-2-macroglobulin, thiol-ester bond-forming	3	3.60E-04
A-macroglobulin complement component	3	4.40E-04

Alpha-macroglobulin, receptor-binding	3	4.40E-04
Alpha-2-macroglobulin, N-terminal	3	5.20E-04
Alpha-2-macroglobulin	3	5.20E-04
Alpha-2-macroglobulin, N-terminal 2	3	5.20E-04
Domain:EGF-like 2; calcium-binding	4	5.60E-04
Complement activation, classical pathway	4	6.60E-04
SM01359	3	8.10E-04
SM01361	3	8.10E-04
Terpenoid cyclases/protein prenyltransferase alpha-alpha toroid	3	8.30E-04
Developmental protein	10	8.80E-04
SM01360	3	9.70E-04

Genes listed here were selected in accordance with Table S2.

Table S4. Sequences of gene-specific primers used in this study

Mouse	**Forward primer**	**Reverse primer**
Glyceraldehyde-3-phosphate dehydrogenase (*Gapdh*)	aactttggcattgtggaagg	ggatgcagggatgatgttct
Actin, alpha 2, smooth muscle, aorta (*Acta2*)	tgtgctggactctggagatg	gaaggaatagccacgctcag
Latent transforming growth factor beta-binding protein-2 (*Ltbp2*)	gcgaatgcaagaacacagaa	aatgctcttccccaacacac
Human	**Forward primer**	**Reverse primer**
Glyceraldehyde-3-phosphate dehydrogenase (*GAPDH*)	cctgcaccaccaactgctta	gtcaaaggtggaggagtggg
Actin, alpha 2, smooth muscle, aorta (*ACTA2*)	aagacagctacgtgggtgac	attttctcccggttggcctt
Latent transforming growth factor beta-binding protein-2 (*LTBP2*)	ggatggacaacagcaaacagc	catcgggaatgacctcctcg

Table S5. Comparison of clinical factors between groups with higher levels (>18 ng/mL) and lower levels (≤18 ng/mL) of serum LTBP2 in patients with idiopathic pulmonary fibrosis

	LTBP2-high	**LTBP2-low**	**p**
	n = 65	**n = 51**	
Age, years	73 (68–78)	68 (63–73)	<0.05
Male	57 (88)	44 (86)	NS
Current or former smoker	52 (80)	44 (86)	NS
Smoking dose (pack-year)	34 (10–50)	40 (20–63)	NS
PaO_2 on room air (Torr)	75 (64–84)	78 (71–88)	<0.05
% predicted FVC (%)	67 (54–84)	83 (69–94)	<0.01
% predicted DLCO (%)	58 (48–79)	67 (54–84)	NS
Serum KL-6 (U/mL)	1105 (773–1705)	864 (515–1231)	<0.05
Serum SP-D (ng/mL)	239 (169–369)	211 (127–274)	NS
Serum LDH (U/L)	238 (209–279)	218 (199–262)	NS

Data are described as n (%) or median (interquartile range). All p values were evaluated by Fisher's exact test or the Mann–Whitney U test as appropriate.

Abbreviations: DLCO = diffusion capacity for carbon monoxide; FVC = forced vital capacity; KL-6 = Krebs von den Lungen-6; LDH = lactate dehydrogenase; LTBP2 = latent transforming growth factor-β binding protein-2; NS = not significant; SP-D = surfactant protein-D.

Supplementary figure legends

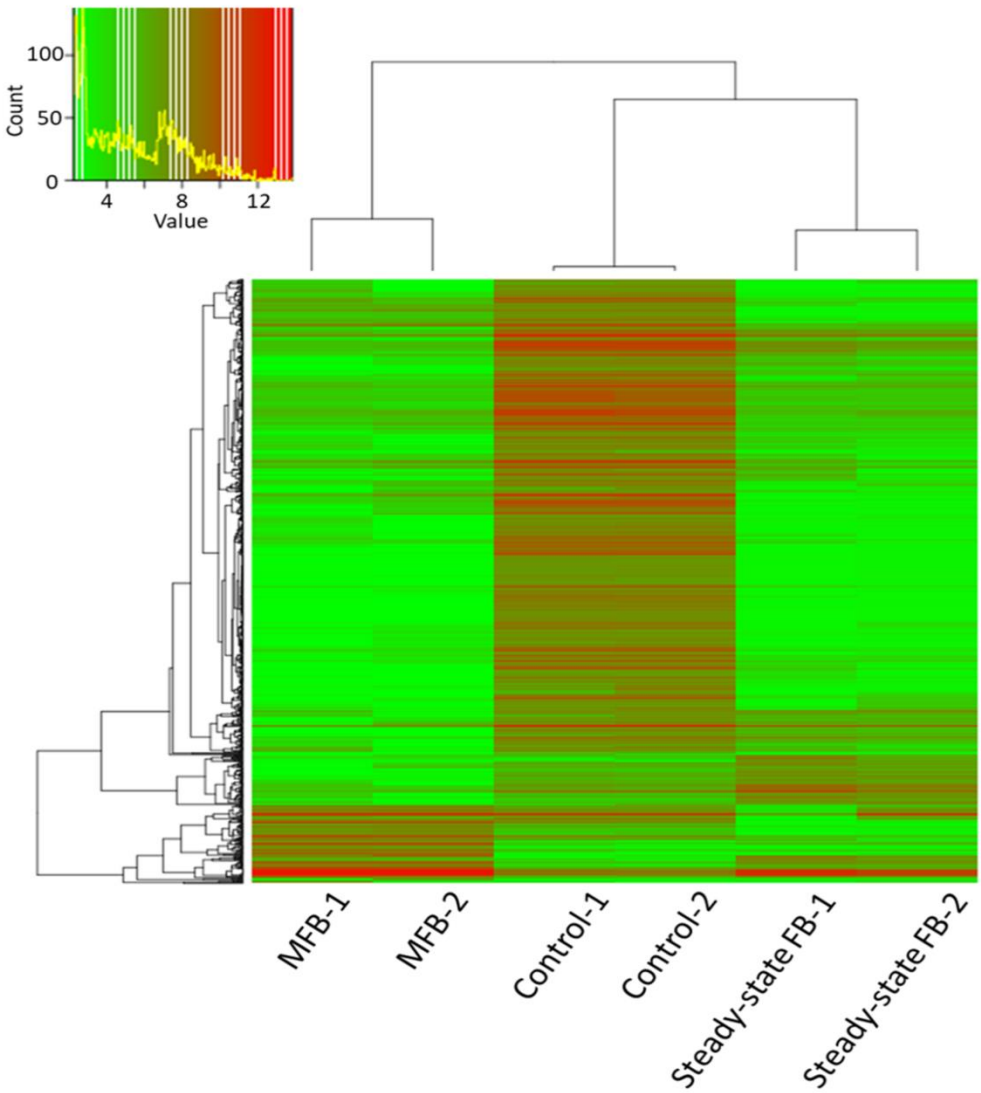

Figure S1. Heatmap of gene expression profiles in each sample

This heatmap is generated using a list of the top 1,000 genes with a large signal gap among all samples (myofibroblasts [MFB], steady-state fibroblasts [FB], and controls). Lung homogenates are used as controls.

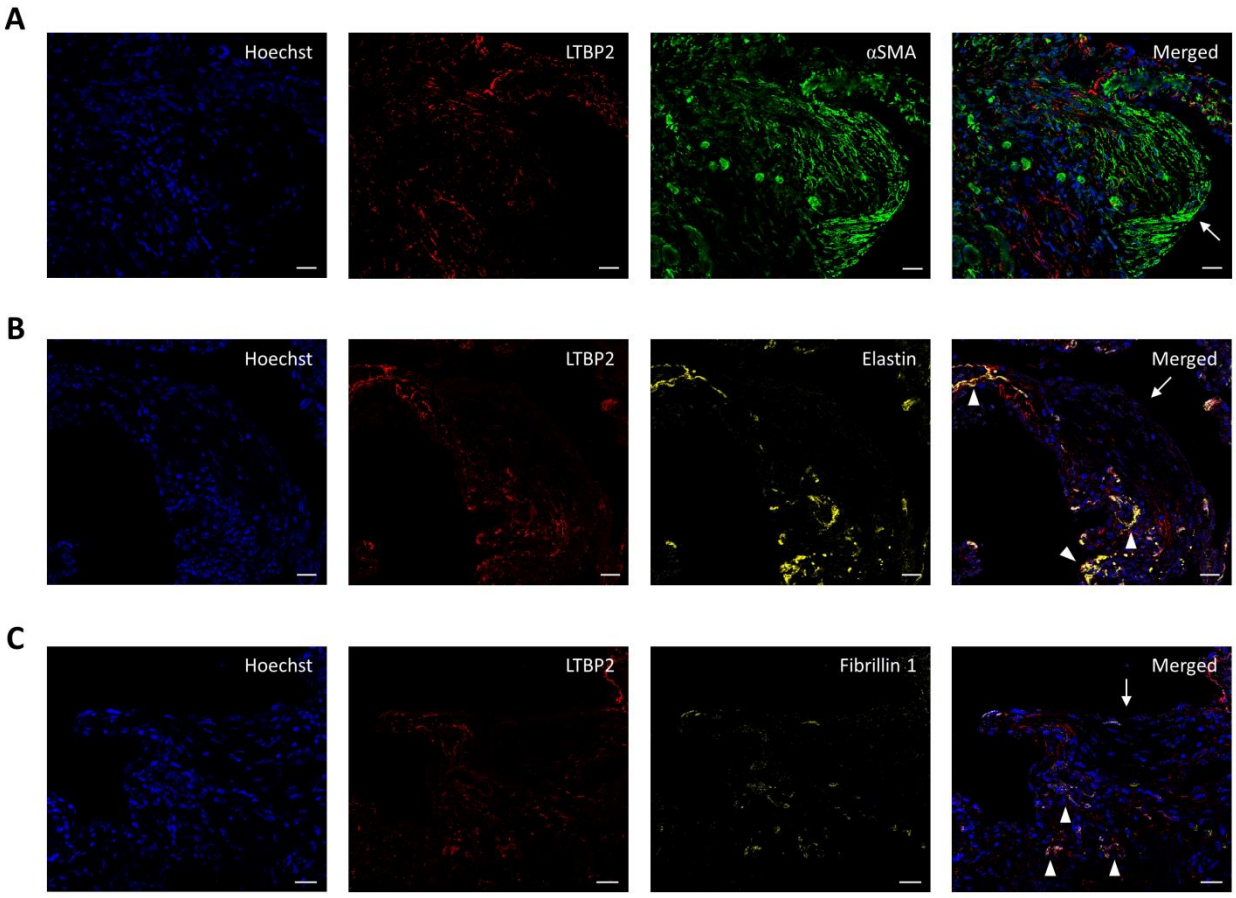

Figure S2. Immunofluorescence images of fibrotic lesions, including fibroblastic foci, in a biopsied lung of idiopathic pulmonary fibrosis

A. Anti-latent transforming growth factor-β binding protein-2 (LTBP2) and anti-α-smooth

muscle actin (αSMA) staining. LTBP2 is broadly upregulated in the fibrotic interstitium but was scarce in the αSMA-positive fibroblastic focus (arrow).

B. Anti-LTBP2 and anti-elastin staining. The positivity of LTBP2 and elastin was partially overlapping (triangles). The fibroblastic focus (arrow) did not show apparent positivity for both proteins.

C. Anti-LTBP2 and anti-fibrillin-1 staining. Similar to elastin, the positivity of fibrillin-1 was also partially overlapping with LTBP2 (triangles). The fibroblastic focus (arrow) did not show apparent positivity for both proteins.

All scale bars = 20 μm.

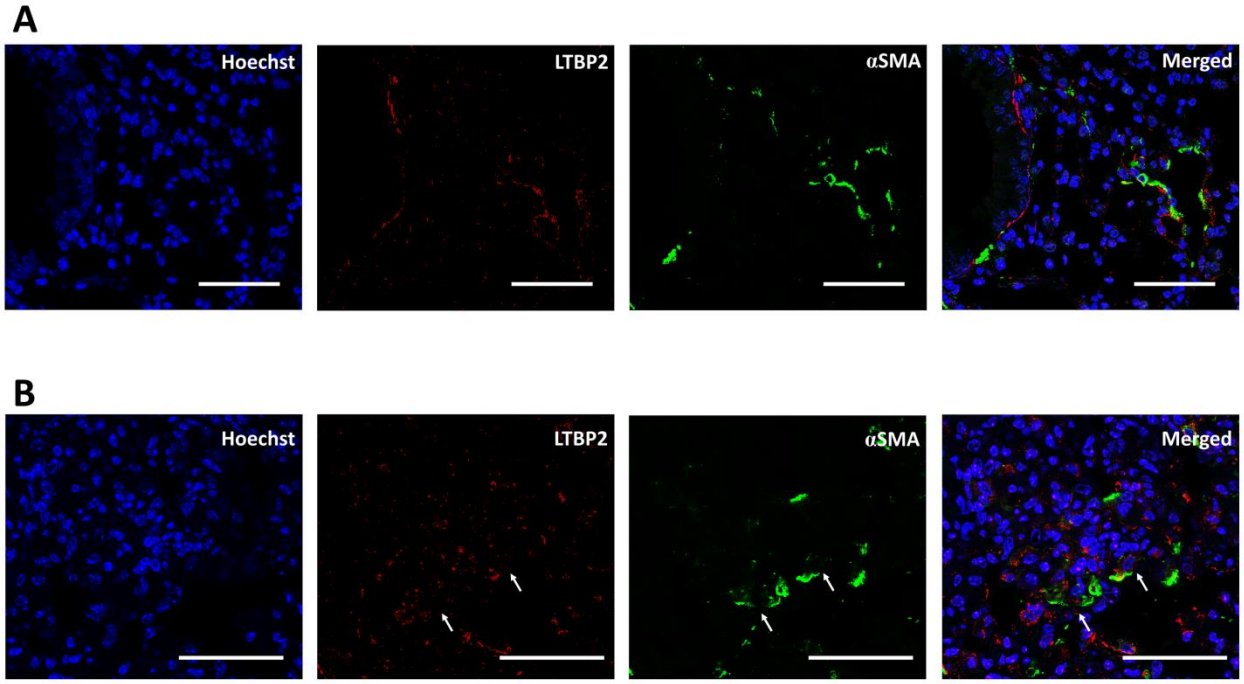

Figure S3. Immunofluorescence images of mouse lungs

A (Untreated mouse lung). Latent transforming growth factor-β binding protein-2 (LTBP2) and α-smooth muscle actin (αSMA) were observed only around the bronchiole and the blood vessel. **B** (Bleomycin-treated mouse lung). LTBP2 positivity was increased in the interstitium mainly as an extracellular matrix protein. Some of the proteins colocalized with αSMA-positive myofibroblasts (arrows).

All scale bars = 50 μm.

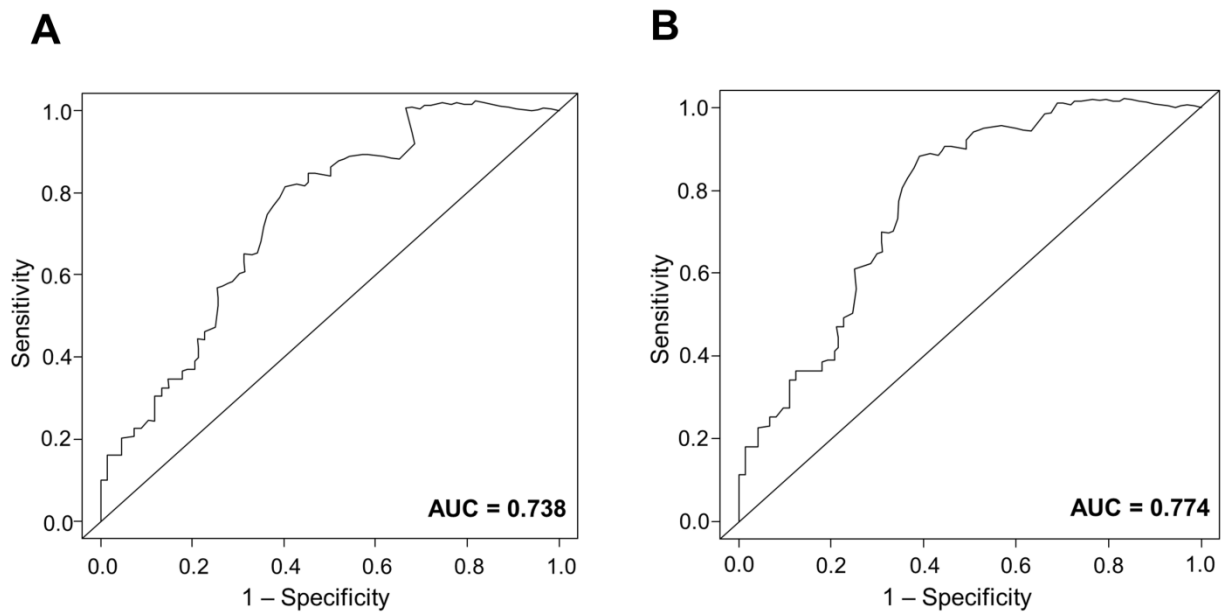

Figure S4. Receiver operating characteristic curves for serum latent transforming growth factor-β binding protein-2 concentrations (evaluated at the time of diagnosis of idiopathic pulmonary fibrosis) during the 60-month follow-up

A. The endpoint was set at all-cause death.

B. The endpoint was set at death by respiratory events.